NASA/CR-1999-208994

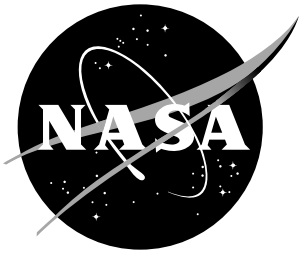

Facesheet Wrinkling in Sandwich Structures

Robert P. Ley, Weichuan Lin, and Uy Mbanefo
Northrop Grumman Corporation, El Segundo, California

January 1999

The NASA STI Program Office ... in Profile

Since its founding, NASA has been dedicated to the advancement of aeronautics and space science. The NASA Scientific and Technical Information (STI) Program Office plays a key part in helping NASA maintain this important role.

The NASA STI Program Office is operated by Langley Research Center, the lead center for NASA's scientific and technical information. The NASA STI Program Office provides access to the NASA STI Database, the largest collection of aeronautical and space science STI in the world. The Program Office is also NASA's institutional mechanism for disseminating the results of its research and development activities. These results are published by NASA in the NASA STI Report Series, which includes the following report types:

- TECHNICAL PUBLICATION. Reports of completed research or a major significant phase of research that present the results of NASA programs and include extensive data or theoretical analysis. Includes compilations of significant scientific and technical data and information deemed to be of continuing reference value. NASA counterpart of peer-reviewed formal professional papers, but having less stringent limitations on manuscript length and extent of graphic presentations.

- TECHNICAL MEMORANDUM. Scientific and technical findings that are preliminary or of specialized interest, e.g., quick release reports, working papers, and bibliographies that contain minimal annotation. Does not contain extensive analysis.

- CONTRACTOR REPORT. Scientific and technical findings by NASA-sponsored contractors and grantees.

- CONFERENCE PUBLICATION. Collected papers from scientific and technical conferences, symposia, seminars, or other meetings sponsored or co-sponsored by NASA.

- SPECIAL PUBLICATION. Scientific, technical, or historical information from NASA programs, projects, and missions, often concerned with subjects having substantial public interest.

- TECHNICAL TRANSLATION. English-language translations of foreign scientific and technical material pertinent to NASA's mission.

Specialized services that complement the STI Program Office's diverse offerings include creating custom thesauri, building customized databases, organizing and publishing research results ... even providing videos.

For more information about the NASA STI Program Office, see the following:

- Access the NASA STI Program Home Page at ***http://www.sti.nasa.gov***

- E-mail your question via the Internet to help@sti.nasa.gov

- Fax your question to the NASA STI Help Desk at (301) 621-0134

- Phone the NASA STI Help Desk at (301) 621-0390

- Write to:
  NASA STI Help Desk
  NASA Center for AeroSpace Information
  7121 Standard Drive
  Hanover, MD 21076-1320

NASA/CR-1999-208994

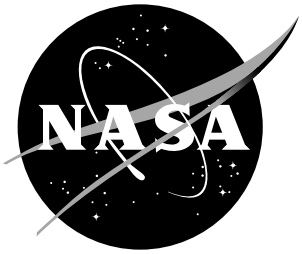

Facesheet Wrinkling in Sandwich Structures

Robert P. Ley, Weichuan Lin, and Uy Mbanefo
Northrop Grumman Corporation, El Segundo, California

National Aeronautics and
Space Administration

Langley Research Center
Hampton, Virginia 23681-2199

Prepared for Langley Research Center
under Contract NAS1-19347

January 1999

Available from:

NASA Center for AeroSpace Information (CASI)
7121 Standard Drive
Hanover, MD 21076-1320
(301) 621-0390

National Technical Information Service (NTIS)
5285 Port Royal Road
Springfield, VA 22161-2171
(703) 605-6000

ABSTRACT

The purpose of this paper is to provide a concise summary of the state-of-the-art for the analysis of the facesheet wrinkling mode of failure in sandwich structures. This document is not an exhaustive review of the published research related to facesheet wrinkling. Instead, a smaller number of key papers are reviewed in order to provide designers and analysts with a working understanding of the state-of-the-art. Designers and analysts should use this survey to guide their judgment when deciding which one of a wide variety of available facesheet wrinkling design formulas is applicable to a specific design problem.

CONTENTS

ILLUSTRATIONS

TABLES

NOMENCLATURE

a	strut or panel length (see Figure 2)
A_0	notch depth (see Figure 19)
b	strut or panel width
D_f	facesheet laminate bending stiffness in the direction of the applied load
D_{11}, D_{12}, D_{22}, D_{66}	facesheet laminate bending stiffnesses
E_c	through-the-thickness Young's modulus of the core
E_f	Young's modulus of the facesheet (isotropic)
F_z	flatwise strength of the core
G_c	transverse shear modulus of the core
k_1, k_2	coefficients in Equations 16 and 17, respectively
K_0	empirically determined constant
L	notch width (see Figure 19)
m	number of wrinkling half-waves (see Equation 15)
P	in-plane load on sandwich strut (see Figure 2)
P_{cr}	critical buckling load
P_E	Euler buckling load
P_s	shear crimping buckling load (see Equation 2)
s	cell size of honeycomb material
t	sandwich thickness
t_c	core thickness (see Figure 2)
t_f	facesheet thickness (see Figure 2)
w^0	initial imperfection shape (see Equation 21)
W	limit of core deformation (see Figure 5)

NOMENCLATURE (CONT'D)

x, y, z	sandwich strut or panel coordinate system (see Figure 2)
δ^0	initial imperfection amplitude (see Equation 21)
λ	buckling mode half-wavelength
λ_{cr}	critical wrinkling half-wavelength
ν	facesheet laminate major Poisson's ratio in the direction of the applied load
ν_c	core Poisson's ratio (isotropic)
ν_f	facesheet major Poisson's ratio (isotropic)
σ_{dimp}	dimpling stress
σ_{wr}	wrinkling stress
σ_x, σ_y	applied compressive stresses in the x- and y- directions, respectively
σ_{wrx}, σ_{wry}	compressive stress allowables in the x- and y- directions, respectively
σ_{wrxy}	smallest of σ_{wrx} and σ_{wry}
σ_z	core flatwise stress
σ_1	major principal compressive stress
σ_{wr1}	major principal compressive stress allowable
σ_2	minor principal compressive stress
σ_{wr2}	minor principal compressive stress allowable
τ_{core}	through-the-thickness shear stress

SECTION 1

INTRODUCTION

The development of fiber composite materials and the drive to reduce both the weight and the cost of aerospace structures has resulted in renewed interest in the use of sandwich construction for primary structures. As considered in this paper, a sandwich structure consists of two thin load-bearing facesheets bonded on either side of a moderately thick, lightweight core that prevents the facesheets from buckling individually. The sandwich structure attains its bending rigidity mainly by separating the facesheets. Solid cores such as those made from foam or balsa wood, or cellular cores such as those made from aluminum honeycomb, may be used. Sandwich structures exhibit very high structural efficiencies (ratio of strength or stiffness to weight). Furthermore, use of sandwich construction in laminated fiber composite applications is particularly attractive since laminated facesheets can be manufactured into complex curved shapes more easily than equivalent metallic facesheets. In addition, with composite materials the facesheet laminates and the facesheet-to-core bond can be cured in a single operation without the need for complex tooling. With sandwich structures the use of discrete stiffening elements can be minimized. Cocuring discrete stiffeners and skins is expensive due to the need for complex tooling; furthermore, these stiffeners give rise to high localized stresses that can be particularly damaging to laminated composite structures.

Sandwich structures with thin facesheets and lightweight cores are prone to a type of local failure known as *facesheet wrinkling* or simply *wrinkling*. Since sandwich structures may exhibit little or no post-wrinkling load carrying capability, failure of these structures by facesheet wrinkling is typically catastrophic. Hence, accurate prediction of facesheet wrinkling is important to the development of reliable and efficient sandwich structures. Throughout this report, the term *wrinkling* refers to modes having wavelengths up to the thickness of the core. The term *buckling* is used in a more general sense, referring to instability modes, regardless of the mode's wavelength.

The purpose of this paper is to provide a concise summary of the state-of-the-art of the analysis for the facesheet wrinkling mode of failure in sandwich structures. The objective here is not to provide an exhaustive summary of all the research related to facesheet wrinkling published in the literature. Instead, the purpose is to present more information from a smaller number of key papers in order to provide designers with a working understanding of the state-of-the-art. Designers and analysts should use this survey to guide their judgment when deciding which one

of a wide variety of available facesheet wrinkling design formulas is applicable to a specific design problem.

This work was performed under Task 13 of NASA Contract NAS1-19347, in support of NASA's Environmental Research Aircraft and Sensor Technology (ERAST) Program. The technical monitor was Mr. Juan R. Cruz.

SECTION 2

ASSESSMENT OF THE STATE-OF-THE-ART FOR PREDICTING FACESHEET WRINKLING FAILURE

This assessment is divided into four sections. Section 2.1 describes the classical approach of treating facesheet wrinkling failure as a short wavelength structural instability. Section 2.2 describes the results of various experiments performed to evaluate the analytical predictions and to calculate necessary "knockdown factors." Section 2.3 describes the treatment of facesheet wrinkling as a strength problem, rather than a stability problem, by considering the presence of manufacturing irregularities (or imperfections). Section 2.4 contains a brief discussion of the effects of combined loads.

2.1 FACESHEET WRINKLING ANALYSES

Facesheet wrinkling has traditionally been treated as a local, short wavelength buckling phenomenon that is one of a number of possible buckling modes exhibited by sandwich structures (see Figure 1). The extremely small buckling wavelength in the wrinkling mode results in the buckling load being insensitive to structural boundary conditions and curvature in all but a few special cases. Many useful theoretical analyses used to predict the onset of wrinkling are based on a mathematical model of the uniaxially loaded flat sandwich strut. Results from the strut analyses are then extrapolated to more complex structures. The usual procedure used to predict the onset of wrinkling in sandwich structures subjected to combined loads starts with the calculation of the maximum principal facesheet compressive stress. This stress is then compared to an allowable stress derived using the uniaxially loaded strut model. For sandwich structures with isotropic facesheets, analytical and experimental evidence (Ref. 1, pp. 44-48) indicates that use of only the maximum principal compressive stress in the facesheet and the wrinkling expressions derived from the strut model results in reasonably accurate wrinkling load estimates.

Consider a sandwich strut loaded in uniaxial compression as shown in Figure 2. The strut is assumed to have a length a, and simply supported at boundary conditions at its ends. The sandwich has facesheets of thickness t_f and a core of thickness t_c. If it is assumed that the core and facesheets have infinite transverse shear rigidities as well as infinite through-the-thickness stiffness, the strut behaves as a classical Euler column. In this case the strut buckles into a mode with half-wavelength equal to the strut length a. A plot showing how the buckling load of the strut, P_{cr}, varies with the buckling mode half-wavelength, λ, appears in Figure 3.

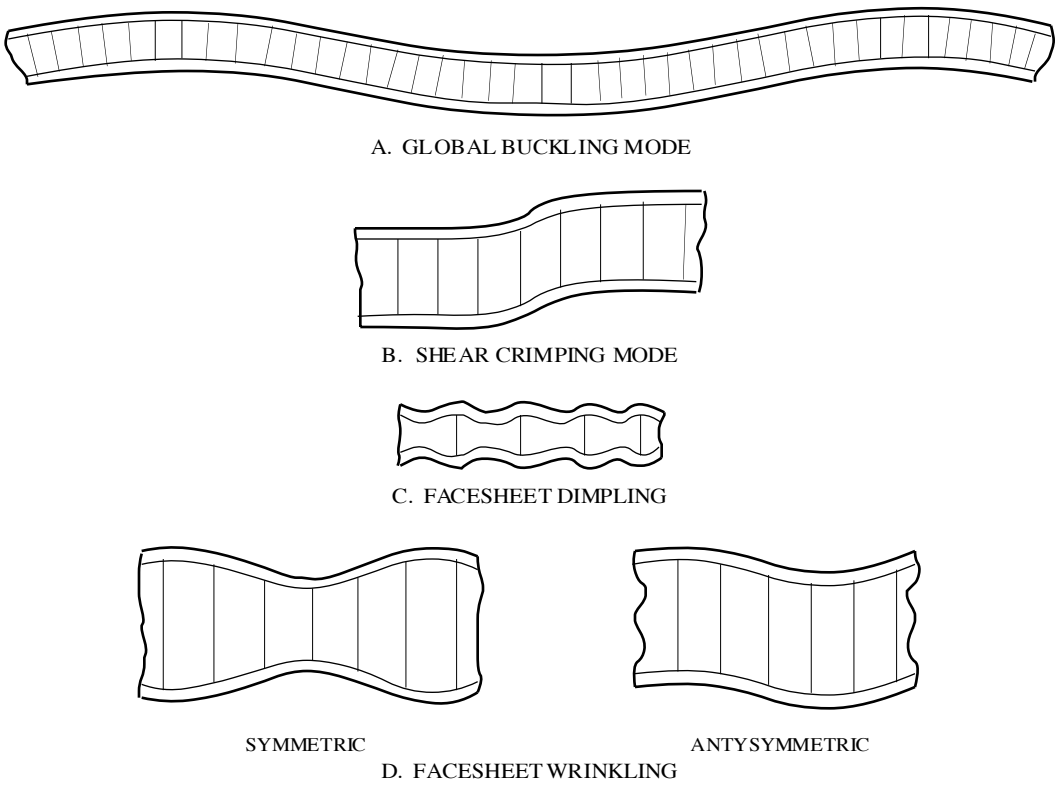

Figure 1. Global and Local Buckling Modes in Sandwich Structures

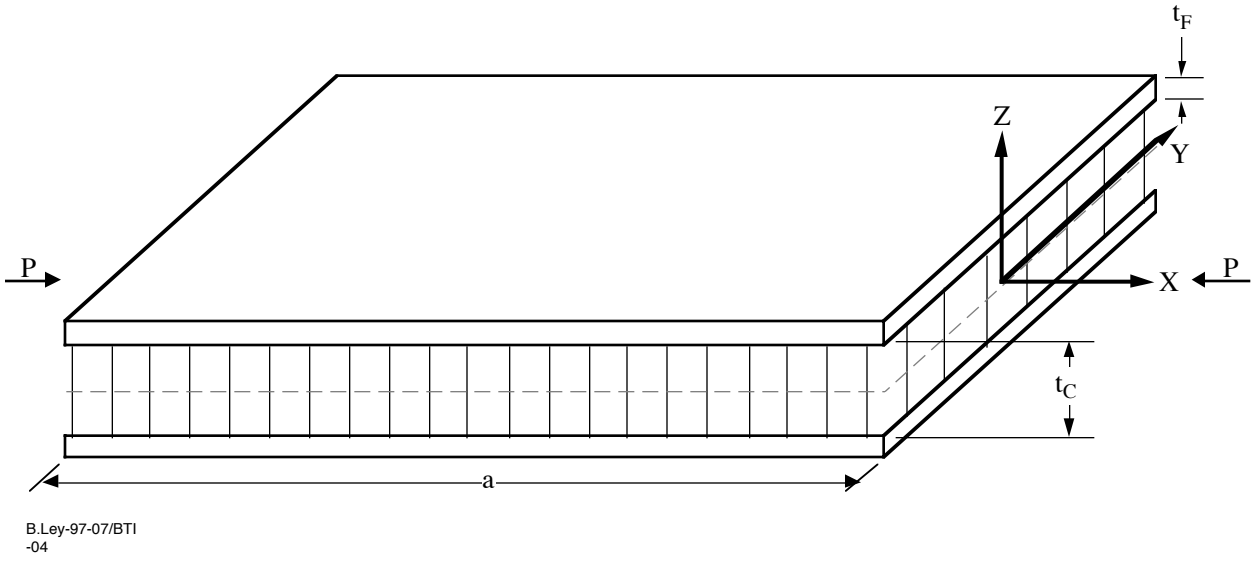

Figure 2. Sandwich Strut Under Uniaxial Load

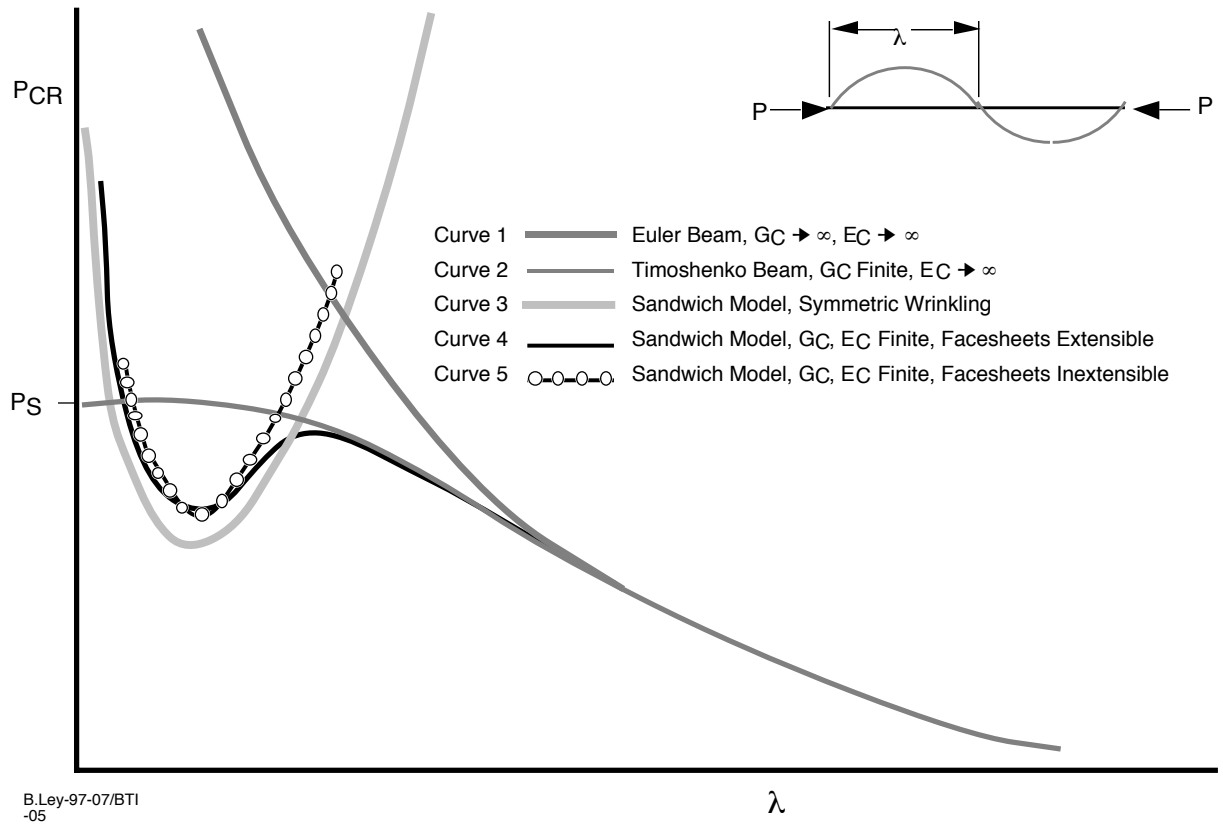

Figure 3. Buckling of a Sandwich Strut

Curve 1 in Figure 3 shows the buckling of the classical Euler column. In most sandwich structures, the transverse shear flexibility of the core is large relative to that of the facesheets and must be considered in the analysis. Treating the sandwich strut shown in Figure 2 as a Timoshenko beam (Ref. 2, pp. 132-135), the buckling load, P_{cr}, can be determined from the following equation

$$\frac{1}{P_{cr}} = \frac{1}{P_E} + \frac{1}{tbG_c} \tag{1}$$

where P_E is the Euler buckling load, t is the thickness of the sandwich, b is the width of the strut, and G_c is the transverse shear modulus of the core. A plot showing how P_{cr} as given in Equation 1 varies with buckling mode wavelength appears as curve 2 in Figure 3. As the wavelength approaches zero, the first term on the right hand side of Equation 1 vanishes leaving

$$P_s = tbG_c \tag{2}$$

This load is usually referred to as the *shear crimping* load in sandwich structures. The shear crimping mode is shown in Figure 1b. Since shear crimping is actually a short wavelength

form of antisymmetric wrinkling, it can be calculated either using Equation 1 with short wavelengths or Equation 2. In general, Equation 1 is generally used for the calculation of buckling loads associated with longer wavelength modes only, while Equation 2 is used for the calculation of the crimping load. Up to this point, somewhat simple expressions have been derived for buckling of the sandwich strut owing to the fact that the through-the-thickness Young's modulus of the core has been assumed to be infinite. The problem becomes substantially more complicated when this assumption is eliminated.

If the through-the-thickness stiffness of the core is considered in the buckling analysis, short wavelength buckling modes, usually known as *facesheet wrinkling modes*, arise. Two facesheet wrinkling cases must be considered. In the first case, the wrinkling of the facesheets is symmetric with respect to the middle surface of the sandwich and can be predicted using the simple model of a plate resting on an elastic foundation. A plot showing how the symmetric wrinkling load typically varies with wavelength appears as curve 3 in Figure 3. In the second case, the facesheets may wrinkle in a mode that is antisymmetric with respect to the middle surface of the sandwich. If the core flatwise stiffness is sufficiently large, wrinkling in an antisymmetric mode does not occur at any wavelength (Ref. 3, p. 188). The symmetric and antisymmetric wrinkling modes are shown in Figure 1d.

Antisymmetric wrinkling is a short wavelength buckling mode of the strut calculated while accounting for the core through-the-thickness and transverse shear flexibilities. A plot showing how the antisymmetric wrinkling load appears as a local minimum at short wavelengths in a plot of buckling load versus wavelength appears as curve 4 in Figure 3. If the end shortening of the facesheets during antisymmetric buckling is neglected (the facesheets are assumed to be inextensible), the resulting approximation cannot be used to predict overall buckling of the strut for long wavelengths. A plot of this approximation to the antisymmetric wrinkling load with respect to wavelength appears as curve 5 in Figure 3.

All of the analyses described up to this point are based upon the assumption that the core provides continuous support to the facesheets. The assumption of continuous facesheet support may not be valid for sandwich structures with honeycomb or other types of cellular cores. In cellular core sandwich structures, if the facesheets are sufficiently thin, the facesheets may buckle locally into the core cells. This type of local instability is known as *facesheet dimpling* (see Figure 1c).

2.1.1 Sandwich Structures With Isotropic Facesheets and Solid Cores

The earliest theoretical studies of the wrinkling of sandwich struts were performed considering only isotropic facesheets and solid, isotropic cores. The first such study was performed by Gough, Elam, and de Bruyne.[4] They assumed that (1) the facesheets were inextensible, (2) the core attached directly to the middle surface of the facesheets, and (3) the effect of the core compressive stresses in the direction of the applied load on the stability of the facesheets could be neglected. Gough, Elam, and de Bruyne[4] considered wrinkling of sandwich struts with the core having the boundary conditions shown in Figure 4. The solution to the problem involved solving the biharmonic equation of elasticity for the core stress function (assuming the core was in a state of plane stress) and enforcing the core boundary conditions. The analysis of Gough, Elam, and de Bruyne[4] as well as their results are summarized on pages 156 through 164 of Reference 3.

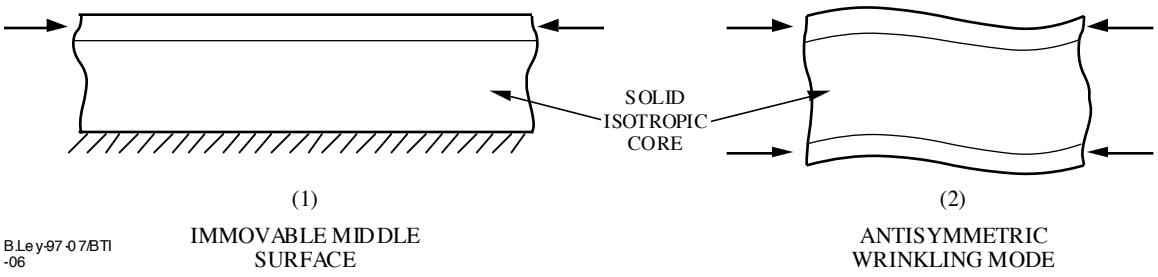

Figure 4. Wrinkling Models of Gough, Elam, and de Bruyne[4]

When the core is sufficiently thick, that is when

$$\left(\frac{t_f}{t_c}\right)\left(\frac{E_f}{E_c}\right)^{1/3} < 0.2 \tag{3}$$

where t_f is the thickness of the facesheet, t_c is the thickness of the core, E_f is the Young's modulus of the facesheet, and E_c is the through-the-thickness Young's modulus of the core, the facesheet can be treated as if it rests on an elastic foundation of infinite thickness. In this case, the stress at which wrinkling would theoretically occur, σ_{wr}, assuming the core Poisson's ratio, ν_c, is zero is given in Reference 4 as

$$\sigma_{wr} = 0.794\left(E_f E_c G_c\right)^{1/3} \tag{4}$$

where G_c is the core transverse shear modulus. Note the lack of dependence of σ_{wr} on the thickness of the core due to the assumption that the core has infinite thickness. For sandwich struts with thinner cores, when

$$\left(\frac{t_f}{t_c}\right)\left(\frac{E_f}{E_c}\right)^{1/3} > 0.2 \tag{5}$$

there is some interaction between the faces on opposite sides of the core. While the theoretical wrinkling load in this case is a function of the core and facesheet properties as shown in Equations 3 and 5, a theoretical lower bound for σ_{wr} that is independent of t_f and t_c for the case where ν_c is zero is given in Reference 3, page 166 as

$$\sigma_{wr} = 0.630\left(E_f E_c G_c\right)^{1/3} \tag{6}$$

The analysis of Gough, Elam, and de Bruyne[4] results in an expression for the wrinkling load that, when plotted, would appear as curve 5 in Figure 3 due to the fact that the facesheets were assumed to be inextensible.

Williams, Legget, and Hopkins[5] were the first to solve the more general problems of antisymmetrical buckling and symmetrical wrinkling of a strut of finite core thickness. Their analysis accounts for the transverse shear and through-the-thickness flexibilities of the core, as well as the stretching of the facesheets. Plots of critical loads calculated using this analysis would be similar to curves 3 and 4 in Figure 3. They also dispensed with the assumption that the core attached to the middle surface of the facesheets but retained the assumption that the effect of the core axial compressive stress on the wrinkling of the facesheets could be neglected. This more general model allowed Williams, Legget, and Hopkins[5] to account for possible interaction of the short wavelength wrinkling mode with the long wavelength buckling mode of the strut. Williams, Legget, and Hopkins[5] concluded that antisymmetric wrinkling always occurred at a lower load than symmetric wrinkling in sandwich constructions with solid, isotropic cores and that the analysis of Gough, Elam, and de Bruyne[4] produced accurate estimates of the small wavelength facesheet wrinkling load. Cox and Riddell[6] present the results of a theoretical study performed using an approach similar to Williams, Legget, and Hopkins[5] in a format more suitable for use in design. For sandwich struts with thick cores, the facesheet wrinkling stress derived by Cox and Riddell[6] is given by

$$\sigma_{wr} = 0.760\left(E_f E_c G_c\right)^{1/3} \tag{7}$$

Hoff and Mautner[7] proposed the simpler models of symmetric and antisymmetric wrinkling for sandwich struts with isotropic facesheets and solid cores depicted in Figure 5. They assumed that core deformations decay linearly to zero within a small zone of width w that is chosen to be the smaller of either one half the thickness of the core or a value that minimizes the facesheet wrinkling stress calculated using a total potential energy formulation. The extensional strain energy of the facesheets, as well as the axial strain energy of the core, are neglected in the formulation; hence, the theory is related to curves 3 and 5 shown in Figure 3. The expressions for σ_{wr} developed by Hoff and Mautner[7] generally depend on the width-to-thickness ratio of the strut. However, based on the specific results presented in Reference 7, the expression for symmetric wrinkling of a sandwich strut with a thick core (one where $w < t_c/2$) provides a reasonable estimate of σ_{wr} in all cases. This value of σ_{wr} is given by

$$\sigma_{wr} = 0.910\left(E_f E_c G_c\right)^{1/3} \tag{8}$$

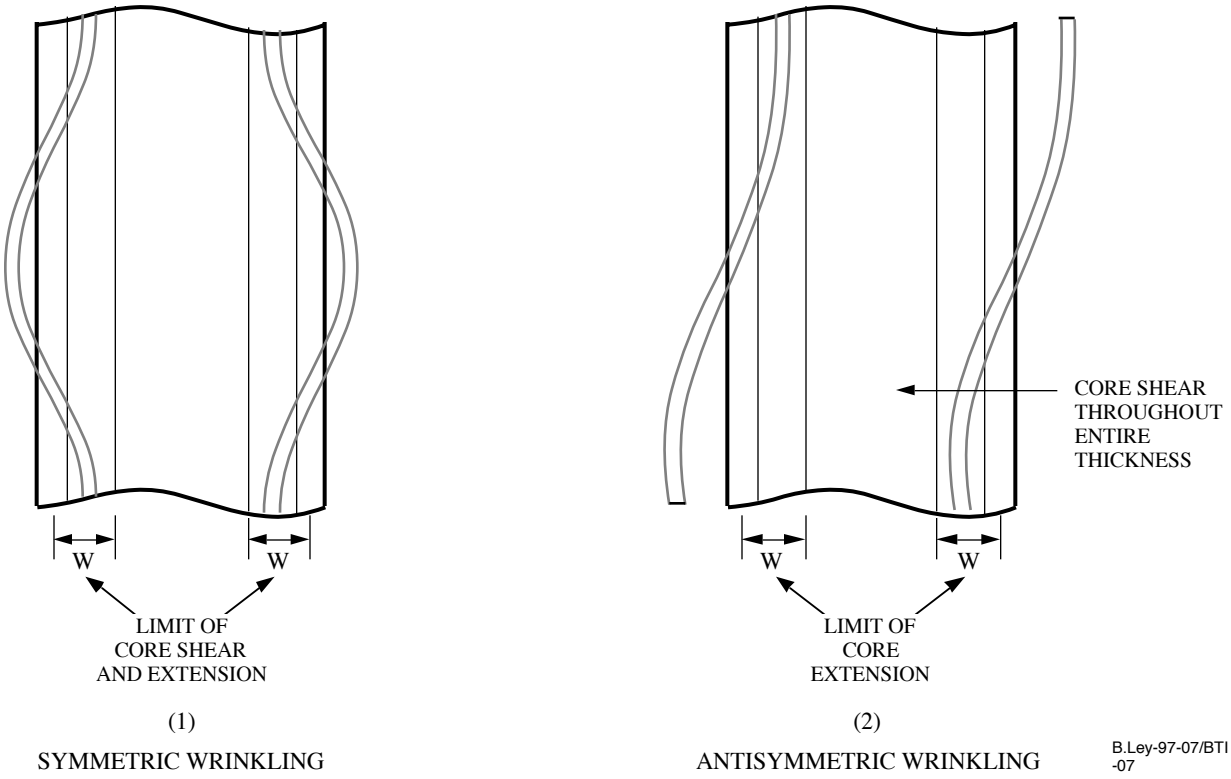

Figure 5. Wrinkling Models of Hoff and Mautner[7]

2.1.2 Sandwich Structures with Isotropic Facesheets and Cellular Cores

Based on his own observations, Williams[8] reasoned that in order for facesheet wrinkling to be a critical failure mode of the sandwich strut depicted in Figure 2, the core-to-facesheet thickness ratio would have to be large enough to render the assumption of a semi-infinite core thickness valid. His analysis is based on the assumption that the axial stress (in the direction of the applied load) in the core was zero. Previous analyses were based on the assumption that this stress was small but nonzero. The assumption of zero core stress in the direction of the applied load is known as the *anti-plane stress assumption* as opposed to the classical plane stress assumption used in the theory of elasticity. This assumption is directly applicable to the analysis of sandwich structures with cellular cores such as honeycomb. Williams[8] assumed the core to be infinitely thick and reasoned that the wrinkling deformations decayed exponentially away from the facesheet into the core. The resulting analysis yielded the following expression for the facesheet stress at which wrinkling would occur:

$$\sigma_{wr} = \left[\frac{0.825}{\left(1-\nu_f^2\right)^{1/3}}\right]\left(E_f E_c G_c\right)^{1/3} \tag{9}$$

where ν_f is the Poisson's ratio of the facesheet.

It can be shown that the form of the wrinkling deformations assumed by Williams[8] result in core stresses that violate the equilibrium equations consistent with the anti-plane stress assumption. A consistent formulation was first presented by Hemp.[9] He considered both symmetric and antisymmetric wrinkling of a sandwich strut having a core of finite thickness. Direct solution of the core equilibrium equations that remain after the anti-plane stress assumption is imposed leads to expressions for the deformations of the core during wrinkling that are simple polynomials in the through-the-thickness coordinate, z (see Figure 2). The wrinkling stress in the symmetric mode presented by Hemp[9] is given by

$$\sigma_{wr} = \left[\frac{0.82E_f}{\sqrt{1-\nu_f^2}}\right]\sqrt{\frac{E_c t_f}{E_f t_c}} \tag{10}$$

Note that a simple beam on an elastic foundation with foundation modulus $2E_c/t_c$ can be shown to have a buckling stress

$$\sigma_{wr} = 0.82E_f\sqrt{\frac{E_c t_f}{E_f t_c}} \tag{11}$$

This purely theoretical value is suggested in Reference 10 for use in the design of sandwich structures with honeycomb cores. After considering the antisymmetric wrinkling mode, Hemp[9] showed that the associated wrinkling stress in sandwich structures with anti-plane cores was 1.732 times higher than the stress associated with wrinkling in the symmetric mode given as written in Equation 10.

Norris et al.[11] extended the analysis of Gough, Elam, and de Bruyne[4] to include allowance for an orthotropic, solid core in either a state of plane stress in the cross section of the core or a state of plane strain. Norris, Boller, and Voss[12] show how, by assuming that the ratio of the core flatwise Young's modulus to core in-plane Young's modulus is infinitely large, the equation for wrinkling stress developed in Reference 11 simplifies to the equation derived by Hemp.[9] Goodier and Neou[13] evaluated the effect of the core axial stress on the wrinkling of the facesheets and verified that it was small by comparing the results of their more general analysis to results published based on the assumption that the effect of core axial stress could be neglected. Addressing the results of some tests indicating panel failure at loads well below those anticipated from wrinkling theory, Goodier and Hsu[14] extended the work of Hemp[9] to include a consideration of wrinkling modes that were not necessarily harmonic in the axial direction. Goodier and Hsu[14] showed that if the ends of the sandwich strut were free to rotate, wrinkling could occur in a mode localized at the ends of the strut (see Figure 6 below) at one-half the load predicted using an analysis based on the assumption of a purely harmonic mode shape.

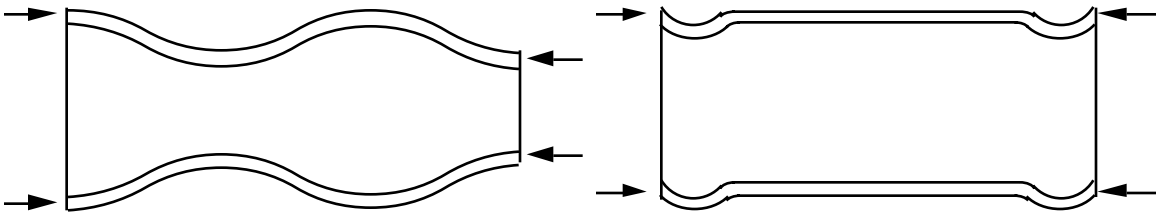

Figure 6. Non-Harmonic Wrinkling Mode in Sandwich Panels

Yusuff[15] combined the anti-plane core assumptions used by Williams[8] and Hemp[9] with the wrinkling model used by Hoff and Mautner[7] to estimate symmetric mode facesheet wrinkling stresses. The expressions for wrinkling stress derived by Yusuff[15] are functions of the calculated width, W (see Figure 5), over which the deformation of the core is assumed to decay linearly to zero. The decay width W is calculated by equating the sum of the core shear and extensional

strain energies stored within the width W to the energy stored in an equivalent extensional spring of modulus K, then minimizing K with respect to W. For thick cores, $W < 0.5t_c$, and

$$\sigma_{wr} = 0.961\left(E_f E_c G_c\right)^{1/3} \tag{12}$$

for thin cores, $W > 0.5t_c$, and

$$\sigma_{wr} = 0.82E_f\sqrt{\frac{E_c t_f}{E_f t_c}} \tag{13}$$

and for cores where $W = 0.5t_c$

$$\sigma_{wr} = 0.82\left(E_f E_c G_c\right)^{1/3} \tag{14}$$

2.1.3 Sandwich Structures With Laminated Composite Facesheets

In the early 1970s, attention focused on sandwich structures fabricated using laminated composite facesheets. The earliest theoretical investigation of facesheet wrinkling with composite facesheets was performed by Pearce and Webber.[16] They extended Hemp's[9] analysis to calculate both symmetric and antisymmetric wrinkling of uniaxially loaded sandwich panels with orthotropic facesheets. They applied the anti-plane core assumptions and accounted for stretching of the facesheets so that long wavelength antisymmetric buckling loads as well as short wavelength antisymmetric wrinkling loads could be calculated using the same analysis. The symmetric wrinkling stress of a sandwich panel with specially orthotropic facesheets was shown to be

$$\sigma_{wr} = \frac{\pi^2}{t_f a^2}\left[D_{11}m^2 + 2\left(D_{12} + 2D_{66}\right)\left(\frac{a}{b}\right)^2 + D_{22}\left(\frac{1}{m^2}\right)\left(\frac{a}{b}\right)^4\right] + \frac{2E_c a^2}{m^2\pi^2 t_f t_c} \tag{15}$$

where the D_{11}, D_{12}, D_{22}, and D_{66} are the facesheet laminate bending stiffnesses, a is the panel dimension in the direction of the applied load, and b is the panel dimension transverse to the applied load. It can be shown that Equation 15 reduces to Equation 10—Hemp's[9] Equation for symmetric facesheet wrinkling—when isotropic facesheets are considered. Webber and Stuart[17] solved the equations of Pearce and Webber[16] for the more general case of sandwich structures with laminated facesheets that exhibit bending-extension coupling; however, they did not present any numerical results.

Gutierrez and Webber[18] extended the analysis of Pearce and Webber[16] to study the facesheet wrinkling of sandwich beams subject to bending. They compared the facesheet stress

on the compressive side of the beam necessary to cause wrinkling to the wrinkling stress calculated based on a uniaxially loaded strut model (both facesheets in compression). For the example presented in Reference 18, the wrinkling stress calculated using the more accurate beam model was approximately 16% higher than the wrinkling stress calculated using the uniaxially loaded strut model. The analysis of Gutierrez and Webber[18] was also general enough to allow for unsymmetrically laminated facesheets and the effect of a facesheet-to-core adhesive layer. They showed that including the effect of a 0.005-in-thick adhesive layer on the theoretical wrinkling stress of a 0.010-in-thick facesheet on a 1.0-in-thick core was to increase this wrinkling stress by 50%. Hence, ignoring the effect of an adhesive layer (if such a layer exists) on the wrinkling stress of sandwich panels with very thin facesheets may be very conservative.

Shield, Kim, and Shield[19] considered wrinkling of an isotropic facesheet resting on a semi-infinite, solid, isotropic core using a two dimensional plane strain elasticity model and compared the wrinkling stresses calculated using this model with those calculated using a model of an Euler beam on an elastic foundation. Their study was the first one of its kind to include the effect of shear deformation of the facesheet in addition to the effect of axial stress in the core. The results generally indicated that the simple beam model provides adequate estimates of the wrinkling stress for thin isotropic facesheets resting on solid cores.

2.1.4 Summary

Theoretical studies performed since 1940 have yielded equations used to design sandwich structures against the facesheet wrinkling mode of failure and are based on one of the three mathematical models indicated in Figure 7. These equations, the model they are based on, and the Reference describing how these equations were derived are listed in Table 1. Generally, the axial compressive stress in the facesheet of a strut (or beam) is given by

$$\sigma_{wr} = k_1\left(E_f E_c G_c\right)^{1/3} \tag{16}$$

for sandwich struts with solid, isotropic cores, or by

$$\sigma_{wr} = k_2 E_f \sqrt{\frac{E_c t_f}{E_f t_c}} \tag{17}$$

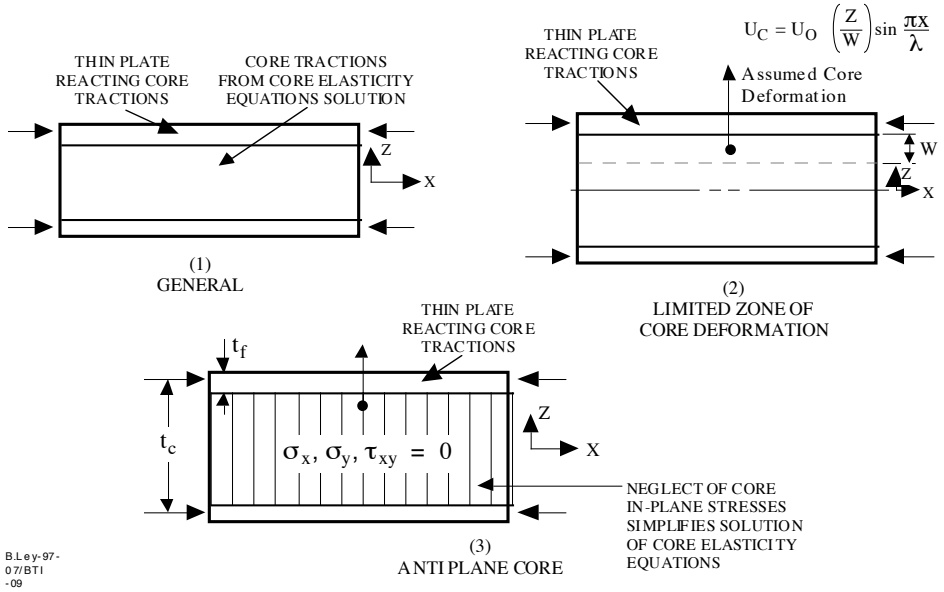

Figure 7. Summary of Facesheet Wrinkling Mathematical Models

Table 1. Summary of Theoretical Wrinkling Stresses For Sandwich Struts With Thick Cores

s_{wr}	MATHEMATICAL MODEL (see Figure 7)	REFERENCE
$0.79\left(E_f E_c G_c\right)^{1/3}$	(1)	Gough, Elam, and de Bruyne[4]
$0.76\left(E_f E_c G_c\right)^{1/3}$	(1)	Cox and Riddell[6]
$0.91\left(E_f E_c G_c\right)^{1/3}$	(2)	Hoff and Mautner[7]
$0.96\left(E_f E_c G_c\right)^{1/3}$	(2)	Yusuff,[15] $W < t_c/2$
$0.82\left(E_f E_c G_c\right)^{1/3}$	(2)	Yusuff,[15] $W = t_c/2$
$0.82 E_f \sqrt{\frac{E_c t_f}{E_f t_c}}$	(2)	Yusuff,[15] $W > t_c/2$
$\frac{0.83}{\left(1-\nu_f^2\right)^{1/3}}\left(E_f E_c G_c\right)^{1/3}$	(2) + (3)	Williams[8]
$\frac{0.82 E_f}{\sqrt{1-\nu_f^2}} \sqrt{\frac{E_c t_f}{E_f t_c}}$	(3)	Hemp[9]

for sandwich struts with cores for which the anti-plane assumption is valid (e.g., honeycomb cores). Equation 17 was derived assuming the core to be in an anti-plane state of stress while Equation 16 was derived without the anti-plane stress assumption. For sandwich structures with orthotropic laminated composite facesheets, an equivalent membrane Young's modulus should not be used. Rather, E_f should be replaced by

$$12\left(1-\nu^2\right)D_f/t_f^3 \tag{18}$$

where D_f is the facesheet laminate bending stiffness in the direction of the applied load. For design purposes, the constants of proportionality k_1 and k_2 have generally been determined experimentally. Experimental results are discussed in Section 2.2.

2.2 EXPERIMENTAL RESULTS

Developing a test to evaluate a highly localized instability failure such as facesheet wrinkling is a difficult task. In this section, facesheet wrinkling stresses determined by tests will be compared to the theoretical values given in Equations 16 and 17. In particular, empirically derived values of the parameters k_1 and k_2 indicated in Equations 16 and 17 will be compared to the theoretical values $k_1 = 0.76$ suggested by Cox and Riddell[6] (thick sandwich structures with solid cores), $k_1 = 0.63$ suggested by Gough, Elam, and de Bruyne[4] (thin sandwich structures with solid cores) and $k_2 = 0.82$ suggested by Yusuff[15] (thick sandwich structures with cellular cores). In order to correlate test measurements with theoretical predictions, it is necessary to ensure that the assumptions made during the theoretical development are valid during the test. A list of some of the more important of these assumptions appears in Table 2. If an assumption is violated in the performance of the test, it is necessary to either design a new test in which the violation is removed or refine the theoretical analysis to allow for the relaxation of the assumption. Whenever possible, test results presented in this section should be evaluated in terms of the relevance of the assumptions listed in Table 2.

2.2.1 Test Results Exhibiting Reasonably Good Correlation With Theoretical Predictions

Hoff and Mautner[7] tested 51 flat, rectangular sandwich panels 4- to 11-in wide and 10.5-in long. These panels were made of 0.006- to 0.02-in-thick laminated paper plastic (papreg) facesheets with a 0.066- to 0.741-in-thick cellulose acetate core. The results of 39 of the 51 tests performed were declared invalid due to premature edge failures caused by insufficient edge support, premature core failure due to the presence of large air bubbles in the core, and

Table 2. Important Assumptions Underlying Facesheet Wrinkling Theoretical Predictions

ASSUMPTION NO.	ASSUMPTION
1	The wrinkling load is independent of boundary conditions and has an associated harmonic mode shape.
2	Symmetric wrinkling failure in sandwich structures always occurs at loads lower than those necessary to cause antisymmetric wrinkling failure.
3	The core provides continuous support to the facesheets.
4	Neither the sandwich nor the individual facesheets exhibit shear-extension, bending-twisting, or membrane-bending material coupling behavior.
5	Any effect of the facesheet-to-core adhesive layer may be neglected.
6	The core may be treated as if it was attached to the middle surface of the facesheets.

difficulties encountered in creating a uniform state of stress in the specimens. Furthermore, test data used to determine the properties of the materials used to fabricate the specimens exhibited extremely high scatter. Using the results of the 12 valid tests and acknowledging the variability in the material properties of their specimens, Hoff and Mautner[7] suggested using a value of k_1 = 0.50 in Equation 16. This value of k_1 is 34% lower than the theoretical value, k_1 = 0.76, suggested by Cox and Riddell[6] for thick core sandwich structures, and 20% lower than the lower bound value, k_1 = 0.63, derived from the work of Gough, Elam, and de Bruyne[4] for thin cores. Note that the formula for the wrinkling stress given in Equation 16 is independent of the core and facesheet thicknesses; it is tacitly assumed that Equation 16 represents a conservative approximation of the true wrinkling stress for all sandwich configurations. The facesheet wrinkling stress given in Equation 16, first proposed in 1945, is widely used today in the design of sandwich structures with solid cores.

Norris et al.[11] tested hundreds of sandwich struts made of various combinations of facesheet and core materials. The facesheets were made of aluminum, steel, and glass cloth laminates. The cores were made of granulated cork, cellular cellulose acetate, balsa wood, and cellular hard rubber. The authors observed four distinct modes of failure during the tests. These failure modes were:

1. Elastic wrinkling of the facesheets at stresses below the proportional limit of the facesheet material
2. Core failure due to “initial irregularities in the facesheets”

3. Core failure at stresses above the proportional limit of the facesheets
4. Compressive strength failure of the facesheets at stresses insufficient to cause facesheet wrinkling.

Since the present focus is on wrinkling failure, the results of tests on specimens that failed in mode (4) are not considered here. As described in Reference 11, the authors observed that the preparation of the specimens that failed in mode (3) was generally poor, yielding unacceptable scatter in the facesheet-to-core bond strength. In addition, several of these specimens failed in an Euler buckling mode. Hence, results from the tests of the specimens that failed in mode (3) will not be considered either.

All specimens made of aluminum and steel facesheets with solid granulated cork cores failed in mode (1)—the failure mode for which the correlation between the theoretically and experimentally determined values of wrinkling stress is expected to be the best. A plot of the wrinkling stresses of the mode (1) specimens, extracted from Tables 2 through 4 of Reference 11, normalized by the facesheet Young's modulus versus $(E_f E_c G_c)^{1/3}/E_f$ appear in Figure 8. The slope of a straight line passing through these data indicates the appropriate value of k_1 to be applied to Equation 16, thus yielding a semi-empirical expression for the facesheet wrinkling stress. As can be seen in Figure 8, the theoretical value of $k_1 = 0.76$ derived by Cox and Riddell[6] for thick solid cores fits the experimental data very well. Furthermore, the theoretical lower bound of $k_1 = 0.63$ derived by Gough, Elam, and de Bruyne[4] for thin solid cores provides a lower bound to the experimental data.

While the specimens that failed in mode (1) were made of solid cork core, the Young's modulus of the cork material was three to four orders of magnitude lower than that of the facesheets. Hence, it is anticipated that the anti-plane core assumptions are valid so that an expression for the facesheet stress of the form shown in Equation 17 is appropriate. A plot of the wrinkling stresses of the specimens that failed in mode (1), extracted from Tables 2 through 4 of Reference 11, normalized by the facesheet Young's modulus versus $(E_c t_f / E_f t_c)^{1/2}$ appears in Figure 9. The slope of a straight line passing through these data indicates the appropriate value of k_2 to be applied to Equation 17, thus yielding a second semi-empirical expression for the facesheet wrinkling stress. As can be seen in Figure 9, the theoretical value of $k_2 = 0.82$ derived by Hemp[9] (assuming $\nu_f = 0$) provides a generally conservative estimate of the wrinkling stresses in these specimens.

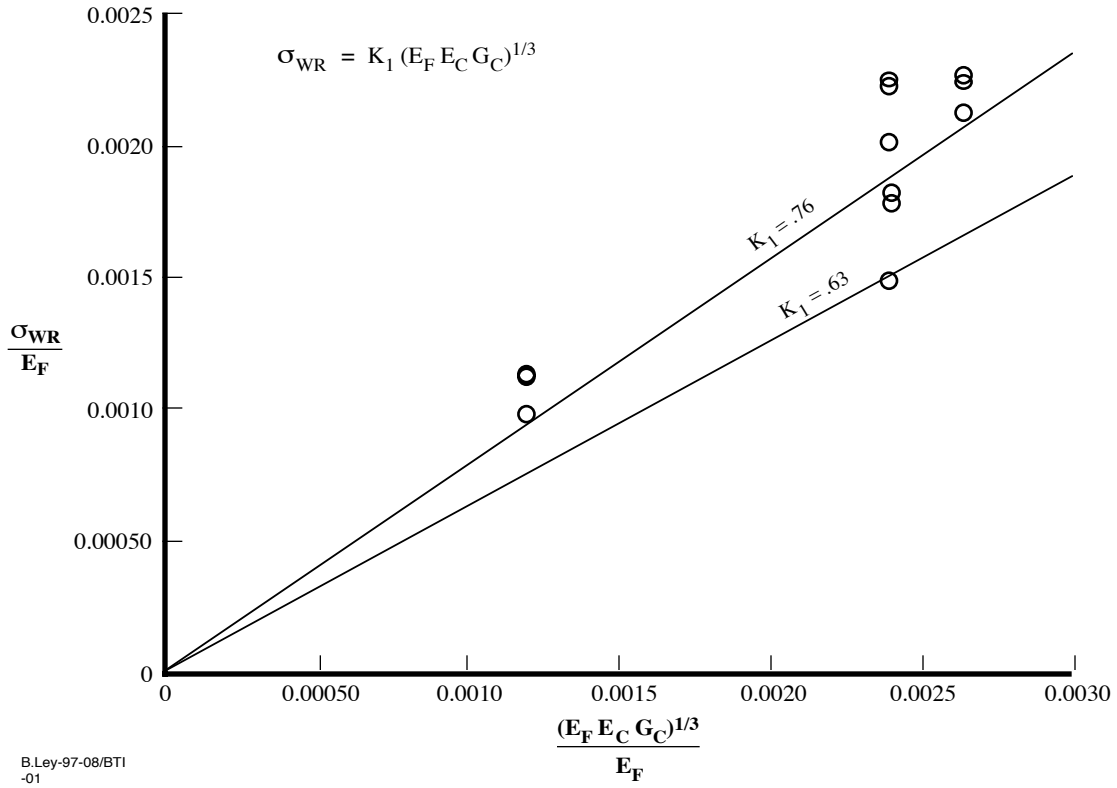

Figure 8. Reference 11 Test Data Mode (1) Failure – Isotropic Core Model

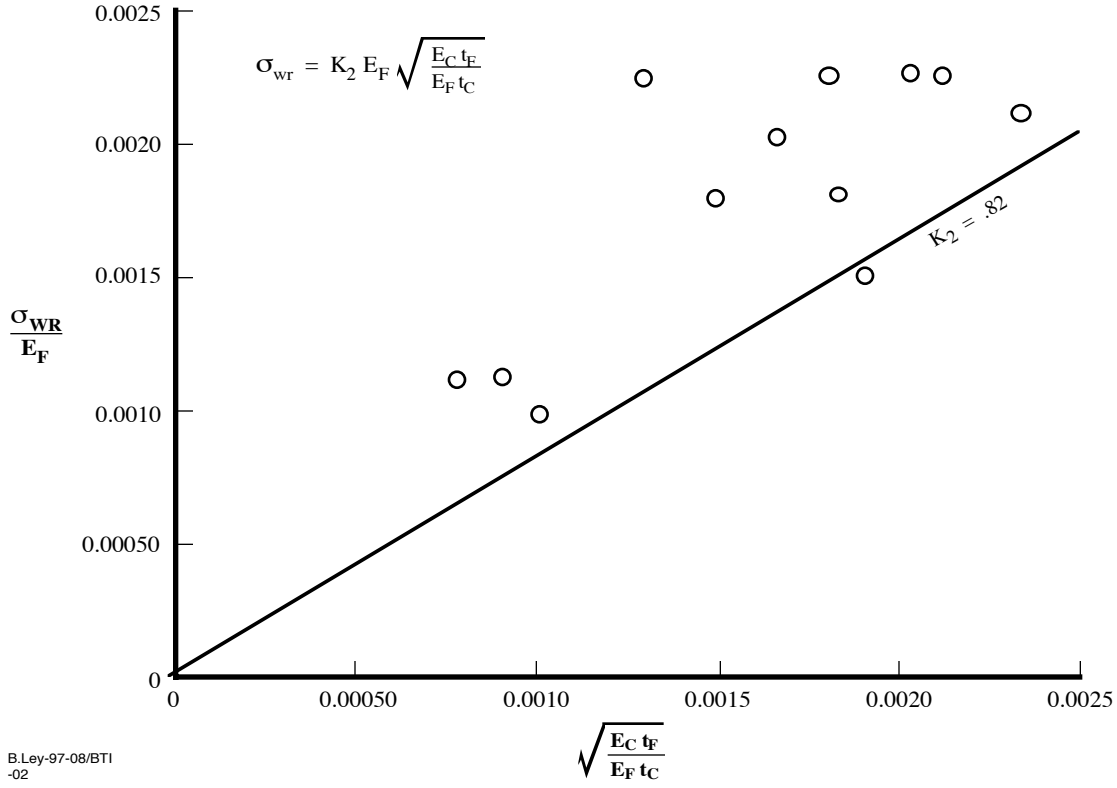

Figure 9. Reference 11 Test Data Mode (1) Failure – Anti-Plane Core Model

The specimens that failed in mode (2) were characterized by failure of the core due to what Norris et al.[11] perceived to be "initial irregularities in the facesheets." A plot of the wrinkling stresses of these specimens, extracted from Tables 6 and 7 of Reference 11, normalized by the facesheet Young's modulus versus $(E_f E_c G_c)^{1/3}/E_f$, appears in Figure 10. A plot of the wrinkling stresses of these specimens normalized by the facesheet Young's modulus versus $(E_c t_f / E_f t_c)^{1/2}$ is shown in Figure 11. The experimentally determined wrinkling stresses are reasonably close to the corresponding theoretical wrinkling stresses except for a single point that represents the wrinkling of the specimen with the smallest (0.25 in) core thickness used. With the exception of this single point, it can be seen from Figure 10 that applying the factor $k_1 = 0.50$ to Equation 16, as suggested by Hoff and Mautner,[7] provided a reasonable lower bound estimate of the wrinkling stress. Similarly, as can be seen from Figure 11, applying the factor $k_2 = 0.60$ to Equation 17 provides another reasonable lower bound estimate of the wrinkling stress.

Norris, Boller, and Voss[12] extended the experimental work performed by Norris et al.[11] to sandwich struts with honeycomb cores. A total of 63 tests were performed on sandwich struts having 0.010-in-thick tempered steel facesheets with 0.375- to 2.00-in-thick honeycomb cores made of resin-treated paper. A plot of the wrinkling stresses of the specimens, extracted from Tables 2 and 3 of Reference 12, normalized by the facesheet Young's modulus versus $(E_f E_c G_c)^{1/3}/E_f$ appears in Figure 12. A plot of the wrinkling stresses of the specimens normalized by the facesheet Young's modulus versus $(E_c t_f / E_f t_c)^{1/2}$ appears in Figure 13. Data are omitted from Figures 12 and 13 in cases where the authors indicated that the specimens failed due to core shear instead of facesheet wrinkling. The slope of a straight line passing through the data plotted in Figure 12 indicates the appropriate value of k_1 to be applied to Equation 16. The slope of a straight line passing through the data plotted in Figure 13 indicates the appropriate value of k_2 to be applied to Equation 17. As can be seen from Figure 12, the theoretical value of $k_1 = 0.76$ results in generally unconservative estimates of the wrinkling stress; however, the theoretical lower bound value of $k_1 = 0.63$ fits the data very well. In Figure 13, it can be seen that the data are fit extremely well by a line having slope $k_2 = 0.82$.

2.2.2 Test Results Exhibiting Generally Poor Correlation With Theoretical Predictions

Further empirical studies of the facesheet wrinkling of honeycomb sandwich panels were performed by Jenkinson and Kuenzi[20] and Harris and Crisman.[21] Jenkinson and Kuenzi[20] tested sandwich panels having 0.012- to 0.031-in-thick aluminum and steel facesheets on aluminum honeycomb cores. They tested six replicates of 28 different configurations for a total of 168

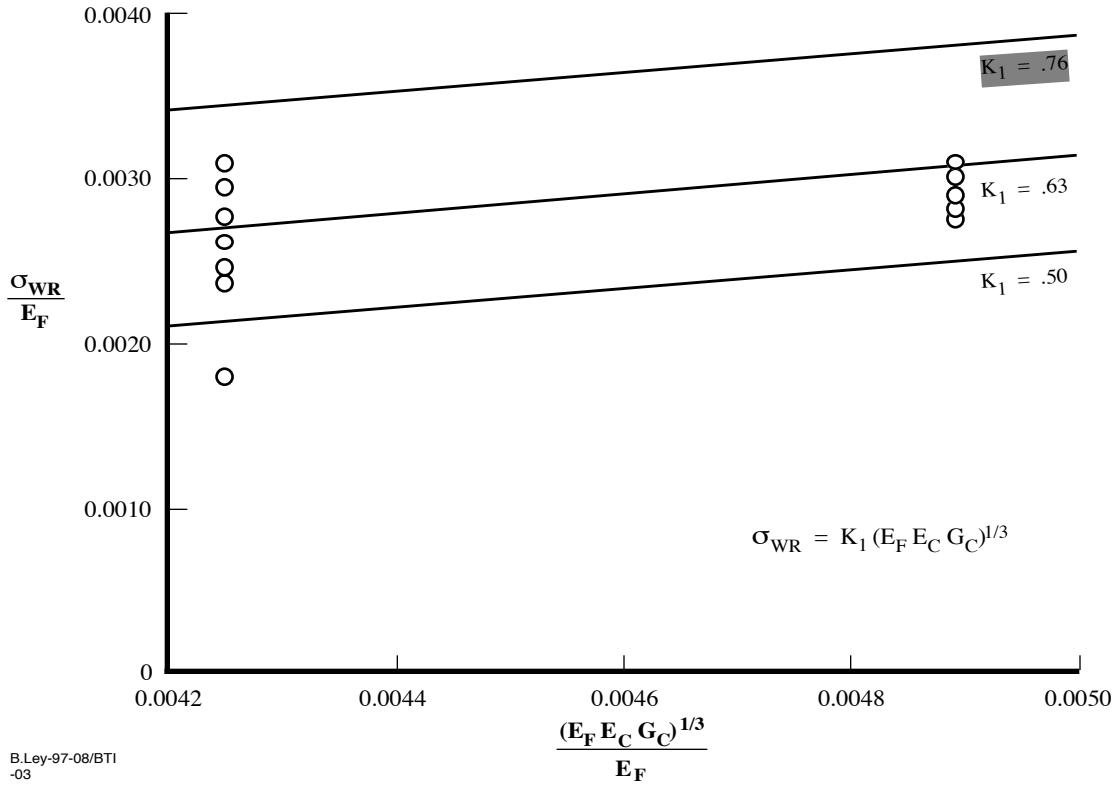

Figure 10. Reference 11 Test Data Mode (2) Failure – Isotropic Core Model

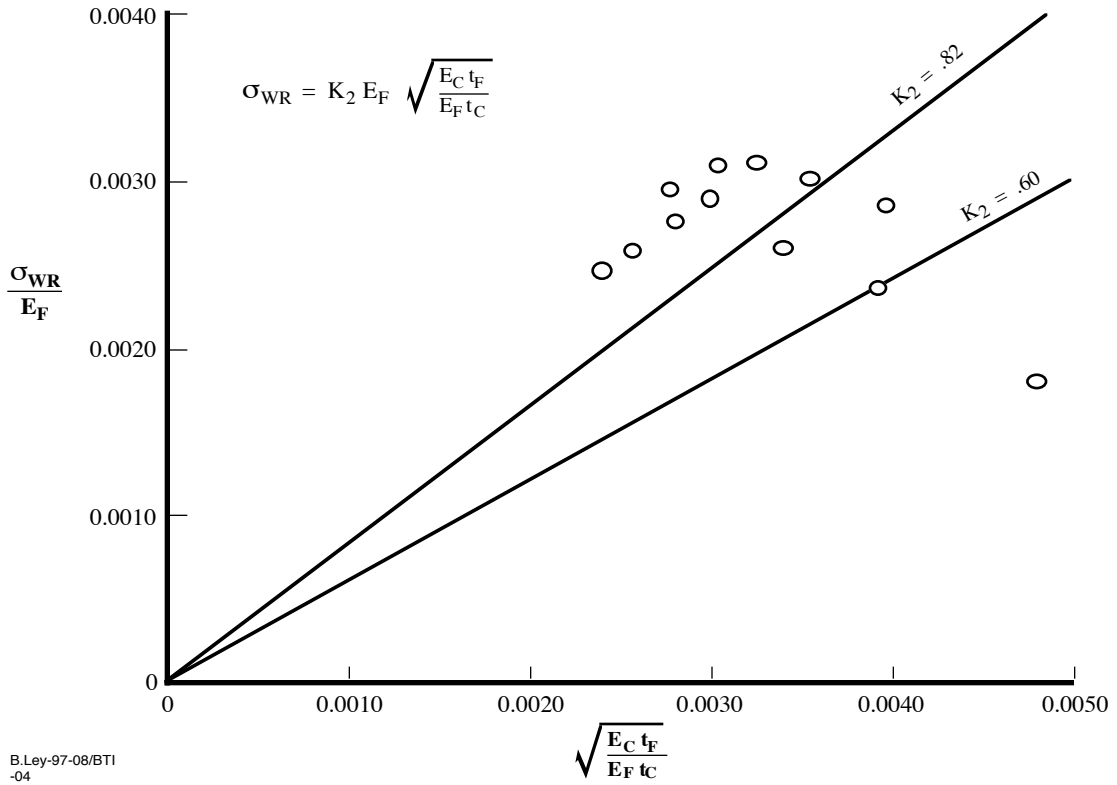

Figure 11. Reference 11 Test Data Mode (2) Failure – Anti-Plane Core Model

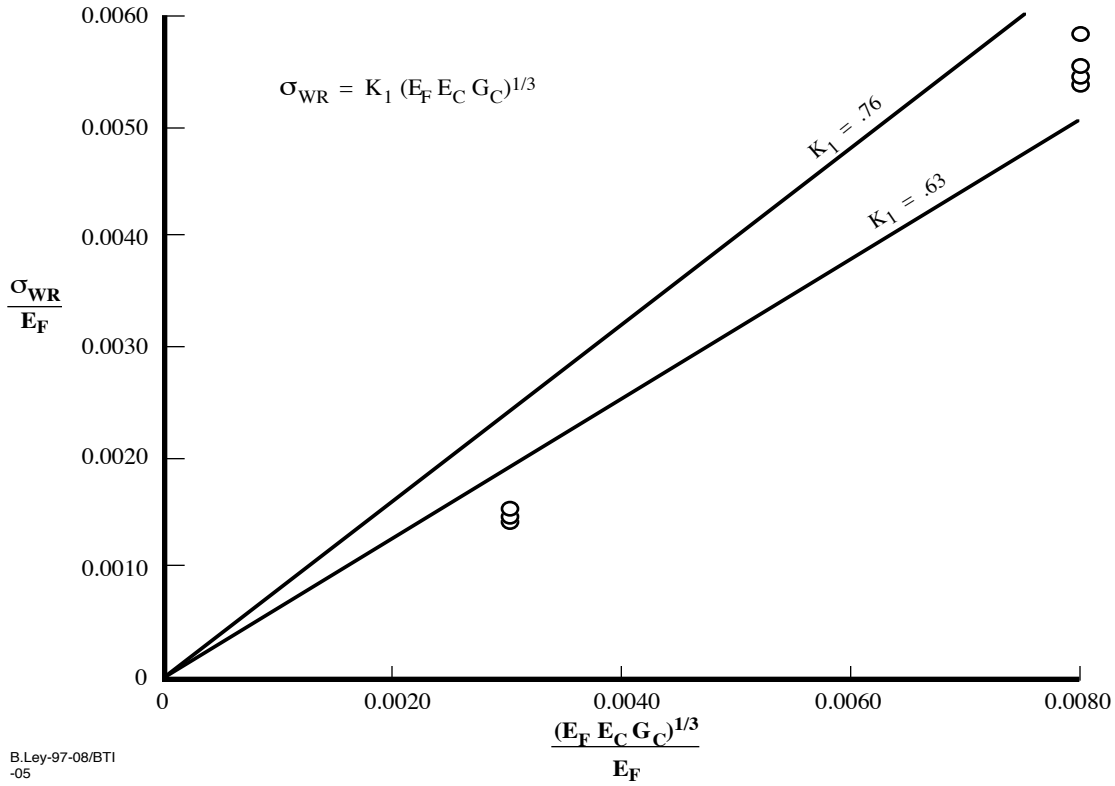

Figure 12. Reference 12 Test Data – Isotropic Core Model

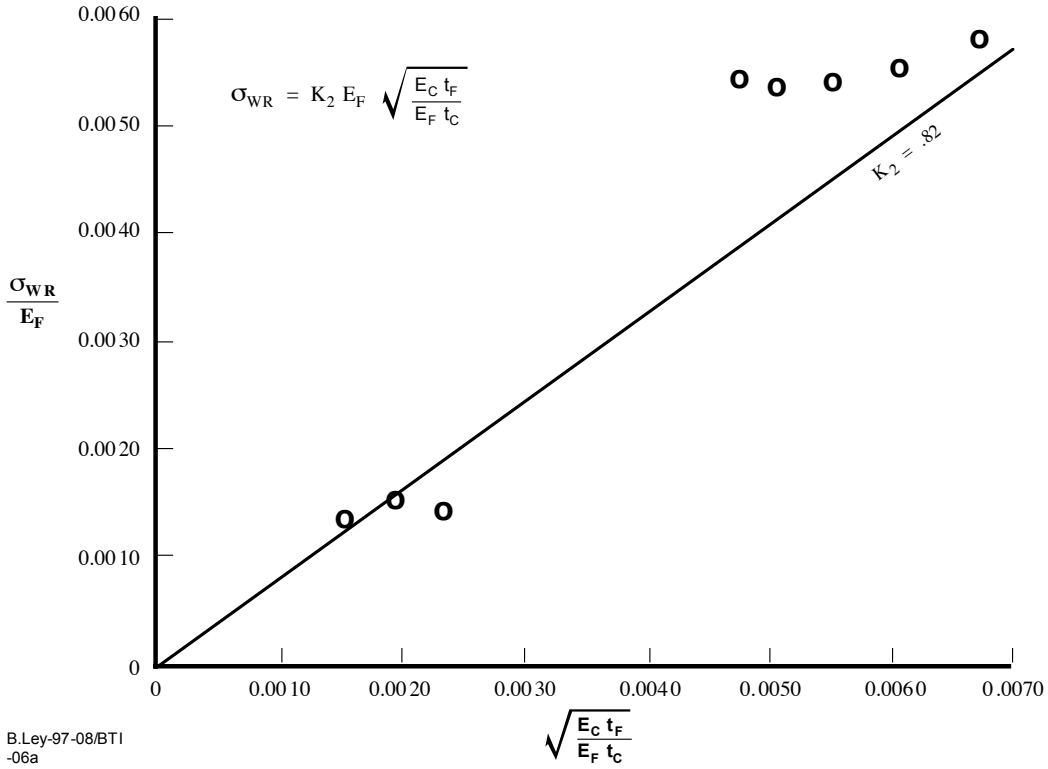

Figure 13. Reference 12 Test Data – Anti-Plane Core Model

tests. Of the 28 different configurations tested, Jenkinson and Kuenzi[20] reported that only 10 configurations failed by facesheet wrinkling away from the loaded ends of the specimens. A plot of the wrinkling stresses of these 10 specimens, extracted from Table 2 of Reference 20, normalized by the facesheet Young's modulus versus $(E_f E_c G_c)^{1/3}/E_f$ appears in Figure 14. A plot of the wrinkling stresses of the specimens normalized by the facesheet Young's modulus versus $(E_c t_f / E_f t_c)^{1/2}$ appears in Figure 15. As before, slopes of best fit lines passing through these data indicate the appropriate value of k_1 to be applied to Equation 16 (Figure 14) or k_2 to be applied to Equation 17 (Figure 15). Jenkinson and Kuenzi[20] suggested $k_1 = 0.044$ as shown in Figure 14. A line of slope $k_2 = 0.125$ fits the data approximately as shown in Figure 15. These values differ substantially from the theoretical values of $k_1 = 0.76$ and $k_2 = 0.82$. Jenkinson and Kuenzi[20] attributed these discrepancies to initial waviness of the facesheets.

Jenkinson and Kuenzi[20] theorized (as did Norris et al.[11] and Norris, Boller, and Voss[12] before them) that the wrinkling load was a function of the facesheet-to-core flatwise strength. They presented data showing that the higher the facesheet-to-core flatwise strength, the higher the facesheet wrinkling stress. Unfortunately, close inspection of the flatwise strength data reported in column 12 of Table 1 of Reference 20 reveals wide scatter in the measured facesheet-to-core flatwise strengths. For example, an average flatwise strength of 90 psi was reported for specimen 20; however, one standard deviation of the test data was equal to 37 psi. Flatwise strengths of some specimens were as low as 20 psi. This is no doubt attributable to the relatively crude facesheet-to-honeycomb adhesive and bonding technology available in the late 1950s when the work was performed. The availability of modern film adhesives and bonding processes has resulted in higher and more repeatable bondline strengths. This more modern technology was used by Harris and Crisman.[21]

Harris and Crisman[21] tested sandwich panels having 0.020- to 0.040-in-thick fiberglass facesheets on 0.40- to 1.00-in-thick aluminum honeycomb cores. Their objectives were to develop a more reliable semi-empirical analysis accounting for initial facesheet waviness and to investigate possible differences in facesheet wrinkling stress when a compressive load is applied normal to the ribbon direction of the honeycomb core versus when it is applied parallel to the ribbon direction. A total of 96 tests were conducted on panels with 18 different configurations. Only average measured wrinkling stress values are presented; the amount of scatter in the test data is not presented in Reference 21. Plots of the measured wrinkling stresses of the specimens, presented in Table 1 of Reference 21, normalized by the facesheet Young's modulus versus $(E_c t_f / E_f t_c)^{1/2}$ for loading parallel and normal to the ribbon direction of the core, appear in

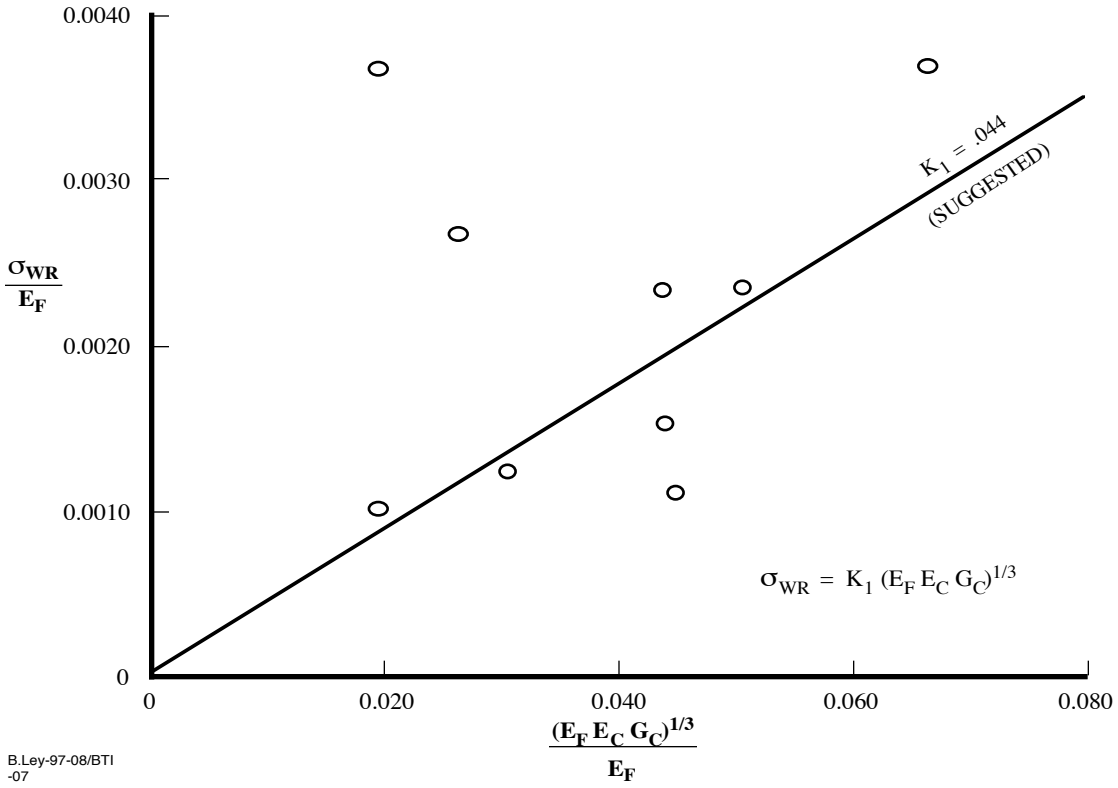

Figure 14. Reference 20 Test Data – Isotropic Core Model

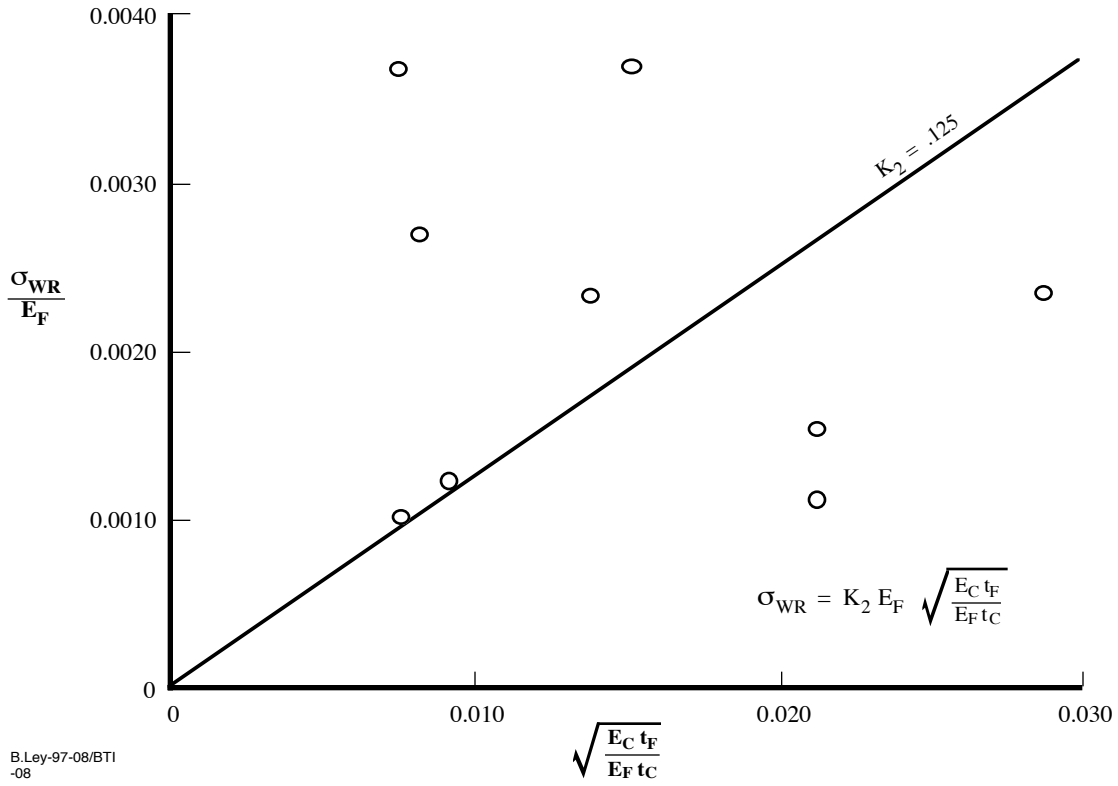

Figure 15. Reference 20 Test Data – Anti-Plane Core Model

Figures 16 and 17, respectively. Straight lines bounding these data also appear in Figures 16 and 17. The slope of a straight line passing through the data plotted in Figures 16 and 17 indicates the appropriate value of k_2 to be used in Equation 17.

Two conclusions can be drawn from Figures 16 and 17. First, both the upper and lower bound values of k_2 indicated in these figures are less than one-half the theoretical value of $k_2 = 0.82$. Second, the wrinkling stresses of the panels loaded normal to the core ribbon direction are, on average, 30% lower than the wrinkling stresses of the panels loaded parallel to the core ribbon direction. Since the only difference in core ribbon versus transverse properties is the core shear modulus, G_c, Harris and Crisman[21] chose the equations derived by Yusuff[15] as opposed to those derived by Norris, Boller, and Voss[12] (similar to the equations derived by Hemp[9]) as the basis of their semi-empirical formulation. This choice was made since the theoretical symmetric mode wrinkling stress equation derived using the theory of Norris, Boller, and Voss[12] was independent of G_c while Yusuff's[15] equation was a function of G_c. Harris and Crisman[21] do not mention the possibility that some of the panels failed in an antisymmetric (core shear) mode rather than a symmetric mode.

Why was the theoretical-experimental correlation of the wrinkling stress of sandwich panels with honeycomb cores reported by Norris, Boller, and Voss[12] so much better than that reported by Jenkinson and Kuenzi[20] and Harris and Crisman[21]? As stated earlier, poor theoretical-experimental correlation is generally attributed to manufacturing imperfections; however, another possible explanation can be found by investigating the theoretical wavelength of the wrinkles more closely. Using the specimen information provided by Norris, Boller, and Voss,[12] Jenkinson and Kuenzi,[20] and Harris and Crisman,[21] the critical wrinkling half-wavelengths of the specimens can be calculated from

$$\lambda = \pi\left(\frac{t_c D_f}{2E_c}\right)^{1/4} \tag{19}$$

Equation 19 is derived in Hemp.[9] The dimpling load of the specimens was also estimated using the following expression suggested in Chapter 4 of Reference 22

$$\sigma_{dimp} = \frac{2E_f}{\left(1-\nu_f^2\right)}\left(\frac{t_f}{s}\right)^2 \tag{20}$$

where s is the cell size of the honeycomb core material. Equation 20 is generally somewhat conservative since it does not take into account the reduction in cell size caused by the fillets formed along the walls of the cells by the adhesive used to bond the facesheet to the core.

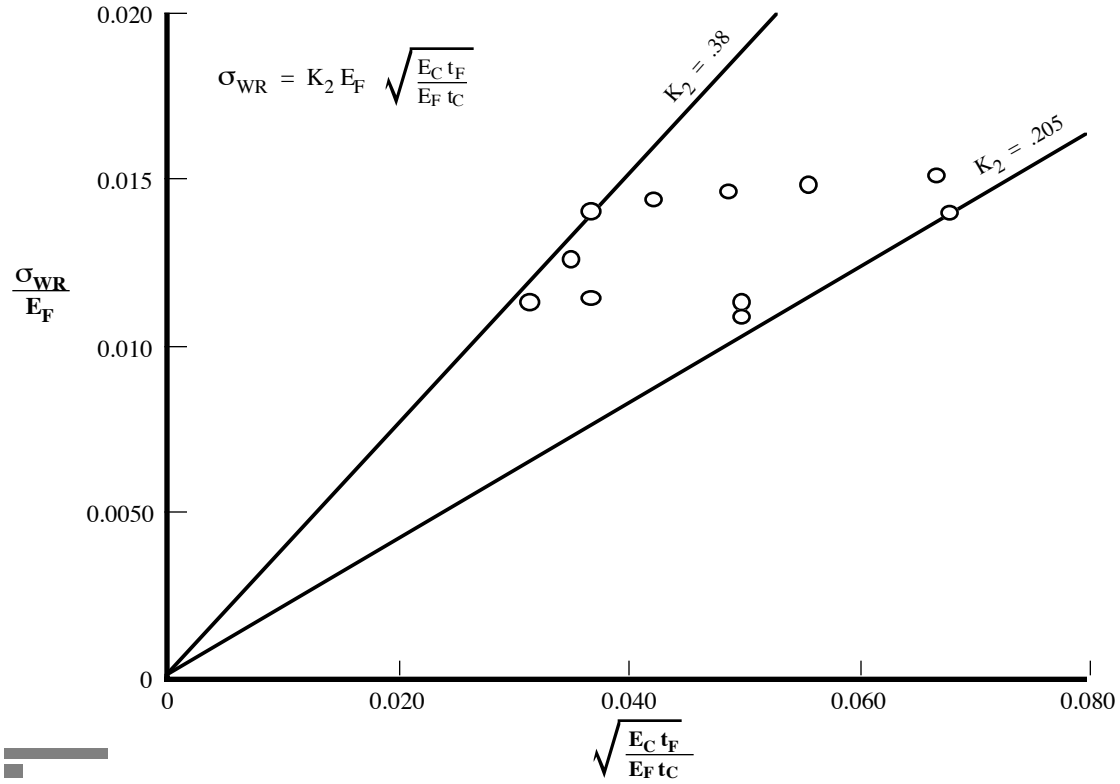

Figure 16. Reference 21 Test Data – Loading Parallel to Core Ribbon Direction

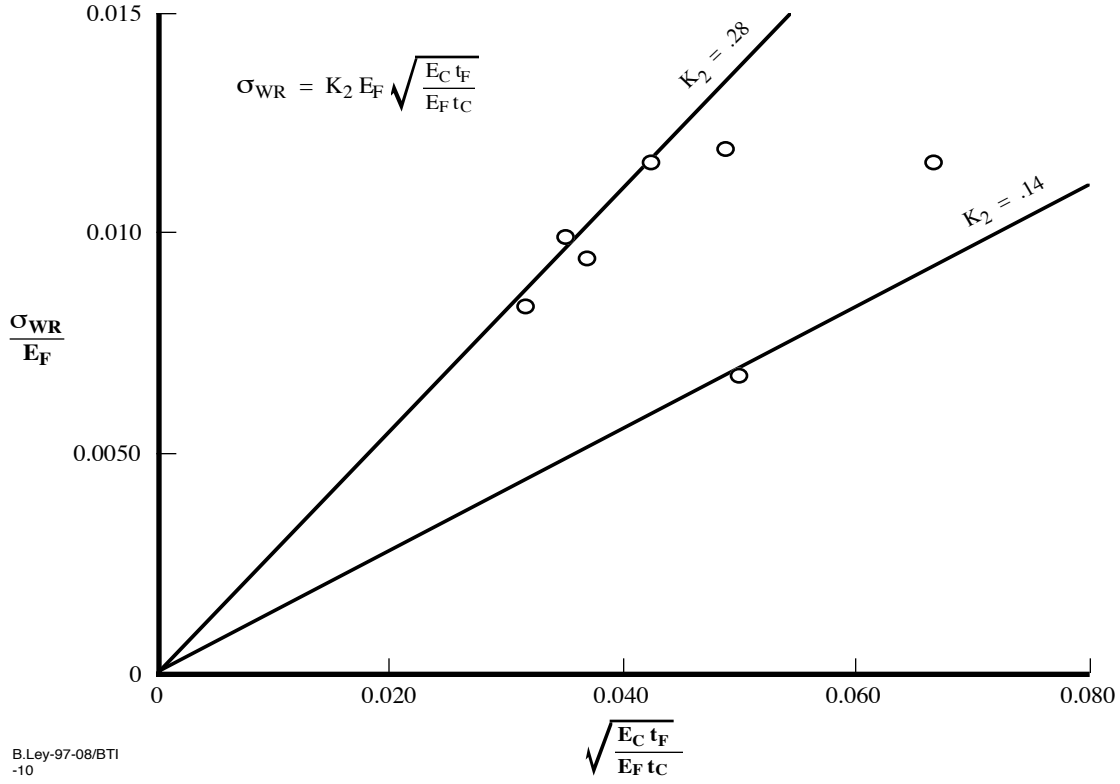

Figure 17. Reference 21 Test Data – Loading Normal to Core Ribbon Direction

Using Equation 19, it was determined that in all of the specimens reported by Jenkinson and Kuenzi[20] and Harris and Crisman,[21] the critical wrinkling half-wavelength was less than the size of a single cell ($\lambda/s < 1.0$); furthermore, the theoretical dimpling stress calculated using Equation 20 was lower than the theoretical wrinkling stress. In cases where $\lambda/s < 1.0$, use of a smeared value of the core flatwise Young's modulus is no longer valid; furthermore, the likelihood of an interaction occurring between the wrinkling and dimpling modes is very strong. A plot of the value of k_2 needed for the expression for wrinkling stress given in Equation 17 to match the various experimental results reported by Norris, Boller, and Voss[12] for specimens with two different core types versus the ratio λ/s appears in Figure 18. This plot indicates that for each specimen set, the larger the ratio λ/s, the more conservative the correlation is between the test data and the theoretical predictions of wrinkling stress. **Hence, it is highly likely that the tests performed by Jenkinson and Kuenzi[20] and Harris and Crisman[21] violated assumption (3) indicated in Table 2.**

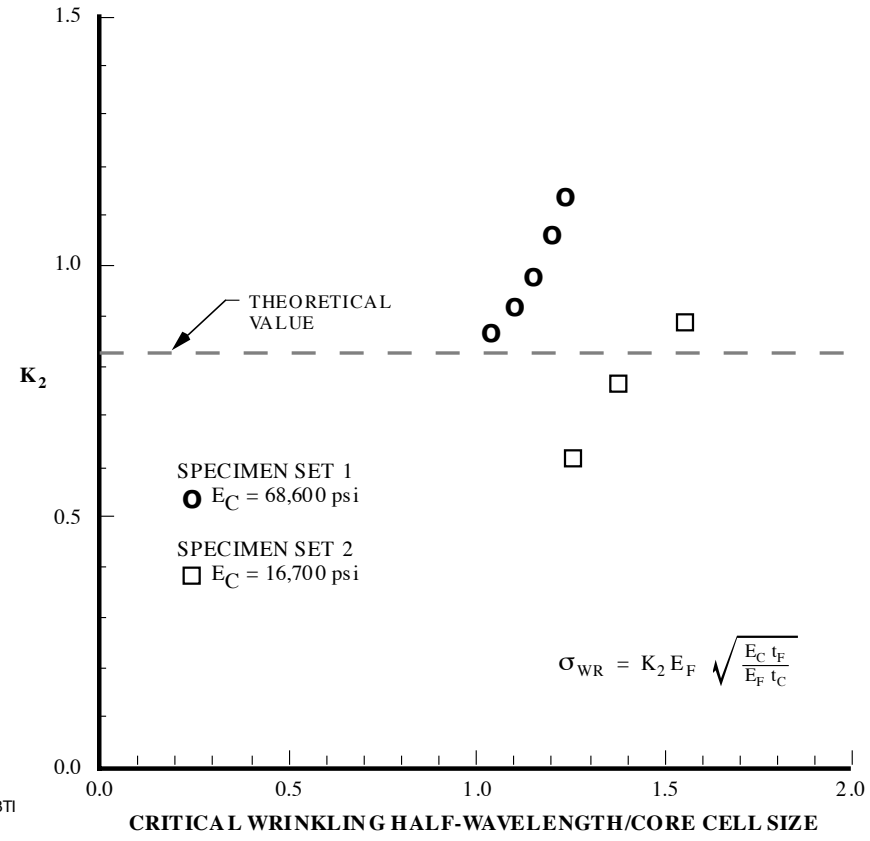

Figure 18. Reference 12 Test Data Plot of k_2 Versus Ratio of Wrinkling Half-Wavelength to Core Cell Size

Another possible explanation for the relatively poor experimental-theoretical correlation of wrinkling stress reported by Jenkinson and Kuenzi[20] and Harris and Crisman[21] is their neglect of the antisymmetric buckling and wrinkling loads. Norris et al.[11] and Norris, Boller, and Voss[12] indicated that many specimens predicted to fail by facesheet wrinkling in fact failed due to shear failure of the core. This could be the result of buckling of the panel in an antisymmetric mode or the presence of initial antisymmetric imperfections. Failure in the antisymmetric mode could certainly explain why Harris and Crisman[21] observed such a marked drop in failure load of specimens loaded normal to the core ribbon direction compared to the failure load of specimens loaded parallel to the core ribbon direction since the antisymmetric buckling load is a function of core shear modulus. **Hence, it is also possible that the tests performed by Jenkinson and Kuenzi[20] and Harris and Crisman[21] violated assumption (2) indicated in Table 2.**

Pearce and Webber[23] tested 10-in-square panels made of 0.01- in to 0.02-in-thick laminated composite facesheets on 0.25-in to 0.500-in-thick aluminum honeycomb cores in edgewise compression. The results of these tests were to be used to validate the theory developed in Reference 16. Since struts tested in previous studies (e.g., References 7, 11, 12, 20, and 21) with support only on the loaded ends were observed to fail catastrophically immediately upon wrinkling of the facesheets, a major objective of the experimental work of Pearce and Webber[23] was to test panels with all four sides supported to see if panels exhibited stable post-wrinkling behavior. Failure of all four of the specimens tested occurred at loads 20% to 30% *higher* than the theoretical (symmetric) wrinkling load but below the theoretical panel buckling load. The authors note that wrinkling of the facesheets was never observed directly; however, strain gauge readings seemed to indicate some form of local instability occurred close to the theoretical (symmetric) wrinkling load. Hence, the authors concluded that wrinkling occurred in isolated areas at loads below the final failure load of the panels indicating that the post wrinkling behavior of the panel was indeed stable. The evidence as to whether or not wrinkling ever occurred was not conclusive. Similar difficulties were encountered during tests performed by Camarda.[24]

Camarda[24] tested 12.0-in-square simply supported panels with 0.024-in-thick quasi-isotropic graphite-polyimide facesheets on 0.50- to 1.00-in-thick glass-polyimide honeycomb cores. A total of nine panels were tested in three different configurations. The results of these tests, along with theoretical predictions of wrinkling stress calculated using Equation 11, appear in Table 7 of Reference 24. Note that the effective facesheet modulus used in the theoretical predictions of wrinkling load (7.538 Msi) does not reflect the true bending stiffness of the facesheet. Using the same laminate theory and material properties used in Section 4.3 of Reference 24, the effective modulus accounting for the bending stiffness of the facesheet rather

than the membrane stiffness is 11.405 Msi resulting in a 23% increase in the theoretical wrinkling loads listed in Table 7 of Reference 24. Based on the new theoretical wrinkling load estimates, it can be seen from Table 7 that the measured wrinkling loads are precisely 50% lower than the theoretical predictions. This is in striking contrast to the results reported by Pearce and Webber.[23] Camarda[24] also states that all of the specimens wrinkled very close to a supported edge. The author went to great lengths in designing a test fixture that would impose no rotational restraint on the panel edges. As pointed out in Section 2.1.2, Goodier and Hsu[14] showed that a nonsinusoidal wrinkling mode can occur near a supported edge at one-half the load predicted by formulas based on the assumption of a sinusoidal mode under such support conditions. Since no mention is made of Goodier and Hsu's[14] work in Reference 24, it is possible that a critical, non-sinusoidal mode was missed. **Hence, it is highly likely that the tests performed by Camarda[24] violated assumption (1) indicated in Table 2.**

Bansemir and Pfeifer[25] conducted a theoretical-experimental study of honeycomb sandwich panels with extremely thin laminated composite facesheets and cores typical of those used in the antennae of modern communications satellites. Their work included tests of panels subjected to pure shear loading, a loading condition absent from every other experimental study previously cited. The authors concluded that an appropriate value for k_2 in Equation 17 is between 0.33 and 0.42. No information about the core cell size of their specimens is provided. Furthermore, the test specimens were all assumed to have failed in a symmetric wrinkling mode based on the authors' calculations indicating that the antisymmetric mode could be neglected. No specific detailed descriptions of the failed specimens are given. Finally, the facesheets themselves were constructed using unsymmetric laminates that exhibit strong bending-stretching coupling. **Hence, the tests performed by Bansemir and Pfeifer[25] violated assumption (4) indicated in Table 2.**

A summary of the correlation of the test results described in this section to the theoretical expressions for wrinkling stress, Equations 16 and 17, appears in Table 3.

2.3 EFFECTS OF INITIAL IMPERFECTIONS

As was mentioned in Section 2.2.2, poor correlation between theoretical estimates and experimental measurement of facesheet wrinkling loads has generally been attributed to initial manufacturing imperfections in the facesheets. These imperfections are random in nature; however, they can be expressed as a linear combination of the facesheet wrinkling mode shapes since these mode shapes are orthogonal. The usual assumption made is that the mode shape

Table 3. Published Test Data Correlation To Theoretical Expressions For Wrinkling Stress

SOURCE	SUGGESTED k_1^*	SUGGESTED k_2^{**}	COMMENTS
Theory	0.76 (upper bound) 0.63 (lower bound)	0.82	—
Hoff and Mautner[7]	0.50	—	Uncertain material properties.
Norris et al.[11]	0.63-0.76	0.82	Nearly perfectly flat facesheets, solid cores.
Norris et al.[11]	0.50	0.60	Imperfect facesheets, solid cores.
Norris, Boller, and Voss[12]	0.63	0.82	Honeycomb cores.
Jenkinson and Kuenzi[20]	0.044	0.125	Tests probably violated assumptions (2) and (3) in Table 2.
Harris and Crisman[21]	—	0.21-0.38 (ribbon direction) 0.14-0.28 (transverse direction)	Tests probably violated assumptions (2) and (3) in Table 2.
Camarda[24]	—	0.41	Tests probably violated assumption (1) in Table 2.
Bansemir and Pfeifer[25]	—	0.33-0.42	Tests violated assumption (4) in Table 2.

$^{*}\sigma_{wr} = k_1\left(E_f E_c G_c\right)^{1/3} \qquad ^{**}\sigma_{wr} = k_2 E_f \sqrt{\frac{E_c t_f}{E_f t_c}}$

corresponding to the lowest wrinkling load is the dominant term in this linear combination. In other words, it is assumed that the undulations of the true surface of the facesheet of a sandwich strut, for example, can be *reasonably approximated* by

$$w^0 = \delta^0 \sin\left(\frac{\pi x}{\lambda_{cr}}\right) \tag{21}$$

where δ^0 is the amplitude of the undulations (waviness), x is the axial coordinate, and λ_{cr} is the critical wrinkling wavelength. Experimental observations indicate that initial imperfections trigger premature failure of the sandwich either by causing a facesheet-to-core flatwise failure (symmetrical imperfections) or a core shear failure (antisymmetrical imperfections).

If a sandwich strut containing an imperfection in the shape of a wrinkling mode is considered, it has been shown that (see, for example Yusuff[26]) the resulting expression for the lateral displacement of the facesheet is

$$w = \frac{\delta^0}{\frac{P_{cr}}{P} - 1} \sin\left(\frac{\pi x}{\lambda}\right) \tag{22}$$

where P is the applied load and P_{cr} is the wrinkling load associated with a wrinkling mode of half-wavelength λ. If the facesheet contains an imperfection in the form of a symmetric wrinkling mode, the maximum facesheet-to-core flatwise stress, σ_z, is given by

$$\sigma_z = \frac{2E_c w}{t_c} = \frac{2E_c \delta^0}{\left(\frac{P_{cr}}{P} - 1\right) t_c} \tag{23}$$

where E_c is the core flatwise Young's modulus and t_c is the core thickness.

If the facesheet contains an imperfection in the form of an antisymmetric wrinkling mode, the maximum core shear stress is (see Reference 1, page 163)

$$\tau_{core} = \left(\frac{t_c + t_f}{t_c}\right) G_c \frac{dw}{dx} = \left(\frac{t_c + t_f}{t_c}\right) \left(\frac{G_c \delta^0 \pi}{\lambda\left(\frac{P_{cr}}{P} - 1\right)} \right) \tag{24}$$

where G_c is the core shear modulus and t_f is the facesheet thickness. If either σ_z exceeds the allowable flatwise stress or τ_{core} exceeds the allowable core shear stress, the sandwich panel will fail.

This assumption of the criticality of imperfections in the shape of the symmetrical wrinkling mode was tested in a controlled fashion by Rogers.[27] The author tested honeycomb sandwich struts with notches intentionally built into the facesheets. As shown in Figure 19, the notch depth, A_0, was known and controlled during the fabrication of the panel. The notch width, L, was then measured following fabrication. Given these two parameters and the critical wrinkling wavelength, λ_{cr}, the value δ^0 could be calculated by a simple ratio. Rogers[27] obtained good theoretical-experimental correlation using this approach given the scatter in the measured values of facesheet-to-core flatwise strength of the test specimens. The results of such a study performed on panels with antisymmetrical imperfections could not be located in the open literature. Various authors have made attempts to estimate δ^0 in Equation 21 based on direct measurements of surface profiles and by comparisons of test data to theoretical predictions.

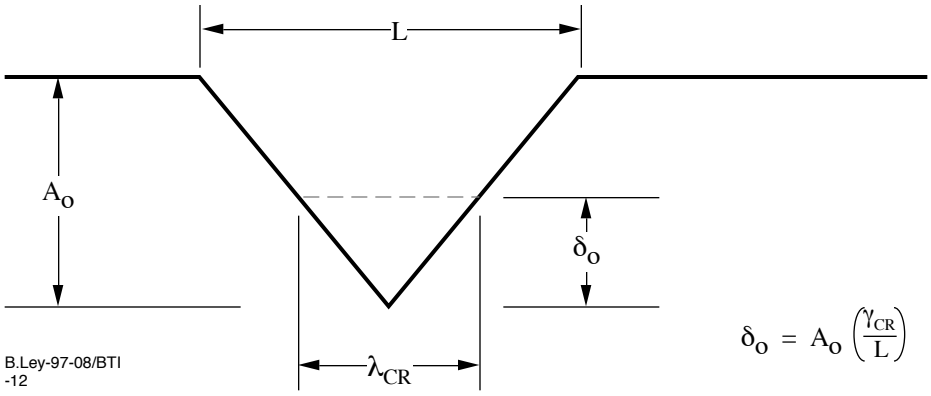

Figure 19. Typical Facesheet Imperfection Manufactured Into Test Specimens in Ref 26

In determining an appropriate value for δ^0, it is reasonable to assume that larger imperfection amplitudes are associated with longer wavelength imperfections. For sandwich constructions with honeycomb cores, Williams[8] suggested that δ^0 was proportional to the wrinkling wavelength, i.e.,

$$\delta^0 = \frac{K_0 \lambda_{cr}}{\pi} \tag{25}$$

where K_0 is a constant to be determined experimentally. Wan[28] suggested that δ^0 was proportional to the square of the wrinkling wavelength and inversely proportional to the facesheet thickness where

$$\delta^0 = \frac{K_0 \lambda_{cr}^2}{\pi^2 t_f} \tag{26}$$

Note that if the wrinkling loads associated with a wide variety of different modes (wavelengths) are not too far apart, Equations 25 and 26 indicate that the assumption of failure in the mode associated with the smallest wrinkling load may be invalid since a mode associated with a higher wrinkling load and longer wrinkling wavelength may have a larger imperfection amplitude.

Norris et al.[11] suggested a different form for the initial imperfection amplitude of sandwich constructions with solid cores. The authors theorized that the waviness was caused by pressure applied during the bonding of the facesheets to the core so that stiffer cores would be more likely to "rebound" from the pressure loading than more compliant cores. Consistent with this idea of core "rebound," Norris et al.[11] found it convenient to define

$$\delta^0 = \frac{K_0 t_c F_z}{E_c} \tag{27}$$

where F_z is the flatwise strength of the core.

Equations 25 through 27 rely on the determination of the constant K_0 by a large number of destructive tests. Test results indicate that all three forms of δ^0 result in reasonably good correlation of theory to test. By assuming that facesheet wrinkling failure occurred when the facesheet-to-core allowable flatwise stress was exceeded, Norris, Boller, and Voss[12] developed the following formula for the facesheet wrinkling stress of sandwich structures with honeycomb cores that includes the effect of initial imperfection:

$$\sigma_{wr} = \frac{0.82}{1 + \delta^0 \left(\frac{E_c}{F_z t_c} \right)} E_f \sqrt{\frac{E_c t_f}{E_f t_c}} \tag{28}$$

Note that Equation 28 is inaccurate if the imperfection precipitates a facesheet fracture failure mode rather than a flatwise stress failure mode. In order to eliminate the need for extensive destructive testing, Norris, Boller, and Voss[12] attempted to directly measure the amplitude of facesheet waviness at the wrinkling wavelength to be used in the theoretical predictions of the wrinkling load and compared the result to a large number of tests. The results were inconclusive. Camarda[24] simply used the largest amplitude available from profile measurements of the panel surface and obtained reasonable correlation between theory and test. As discussed in Section 2.2.2, however, it is likely that the neglect of boundary effects was responsible for the poor correlation between theory and test obtained by Camarda.[24]

Instead of calculating the critical wrinkling load and wavelength, Harris and Crisman[21] simply assumed that the facesheet wrinkled with a wavelength equal to the cell size of the honeycomb core. They developed an empirical expression for the waviness parameter, δ^0, appearing in Equation 28 using the results of a large number of destructive tests. This "curve fitting" technique allowed Harris and Crisman[21] to obtain very good correlation between theory and test. However, as discussed in Section 2.2.2, it is possible that other phenomena, not accounted for in the derivation of Equation 28, may have been responsible for the initially poor correlation of test data with theoretical wrinkling stress predictions made using Equation 17 with $k_2 = 0.82$.

A note of caution is warranted here. Expressions such as that given in Equation 28 are based on the assumption of criticality of imperfections in the symmetric wrinkling mode. However, imperfections in an antisymmetric mode should not be ignored. In Equation 24, it can

be seen that the core shear stress generated in a panel with an antisymmetric imperfection is inversely proportional to the imperfection wavelength, λ. For small values of λ, very high core shear stresses may be generated. Consider shear crimping. In Figure 3, the shear crimping load, P_s, is associated with a zero wavelength, which is of course not possible. In reality, shear crimping is actually a sudden core shear failure triggered by an antisymmetric imperfection. Depending on the magnitude of this imperfection, this core failure may occur at loads substantially below the classical shear crimping load given in Equation 2.

2.4 EFFECTS OF COMBINED LOADS

A rigorous treatment of the wrinkling of sandwich panels subjected to combined loads is conspicuously absent from the literature. As discussed in Section 2.1, Plantema[1] showed that for panels with isotropic facesheets, only the largest principal compressive stress need be considered. Others suggest taking allowable wrinkling stresses measured from tests of uniaxially loaded struts and using them in interaction equations. When the two principal stresses are compressive, it is suggested in Reference 29 that the following interaction equation be used

$$\left(\frac{\sigma_1}{\sigma_{wr1}}\right)^3 + \left(\frac{\sigma_2}{\sigma_{wr2}}\right) = 1 \tag{29}$$

where $\sigma_1$and σ_{wr1} are the major principal compressive stress and the corresponding allowable wrinkling stress and σ_2 and σ_{wr2} are the minor principal compressive stress and the corresponding allowable wrinkling stress. Bruhn[30] suggests always working with stresses rotated into a coordinate system with axes parallel to the core ribbon and transverse directions, then applying the interaction equation of the form, ignoring facesheet plasticity effects

$$\frac{\left(\sigma_{xx}^3 + \sigma_{yy}^3\right)^{1/3}}{K\sigma_{wr}} + \left(\frac{\tau_{xy}}{\sigma_{wr}}\right)^2 = 1 \tag{30}$$

where σ_{xx} and σ_{yy} are the in-plane normal stresses such that the x direction is aligned with the direction of the greatest compressive stress, τ_{xy} is the applied shear stress, σ_{wr} is an allowable wrinkling stress for panels loaded in uniaxial compression along the core ribbon direction, and K=1.0 if the axis of the largest applied compressive stress is parallel to the core ribbon direction, else K=0.95 if it is not parallel to the core ribbon direction.

SECTION 3

CONCLUDING REMARKS

There has been extensive analytical and experimental treatment of the problem of predicting facesheet wrinkling in sandwich structures subjected to compressive loads. Wrinkling can occur either in a symmetric or antisymmetric mode shape as shown in Figure 1. Analyses have been developed based upon two different treatments of the response of the core. The first treatment involves a rigorous solution of the core elasticity equations. This treatment is most applicable to sandwich structures made with solid, isotropic cores and results in an expression for the theoretical wrinkling stress of a uniaxially loaded strut of the form shown in Equation 16 where k_1 is in general a function of the facesheet and core thicknesses and Young's moduli. Other derivations based on assumed core displacement functions that decay exponentially away from the facesheets or that decay linearly to zero over a small region adjacent to the facesheets also lead to theoretical expressions for the wrinkling stress of the form shown in Equation 16.

The second main analytical treatment of the facesheet wrinkling problem involves use of the anti-plane core assumptions. It is assumed that the stresses in an anti-plane core of a sandwich panel in the plane of the applied loads are exactly zero. It has been shown theoretically that sandwich constructions with anti-plane cores always wrinkle at a lower stress in the symmetric mode than in the antisymmetric mode. The expression for the theoretical wrinkling stress (symmetric mode) of a uniaxially loaded sandwich strut with an anti-plane core is of the form shown in Equation 17 where k_2 is a constant.

The results of hundreds of tests of uniaxially loaded sandwich struts with isotropic facesheets and both solid and honeycomb cores conducted to determine facesheet wrinkling loads have been reported in the open literature. The results of far fewer wrinkling tests on panels with anisotropic facesheets subjected to combined loads and supported on all four edges have been published. These tests are extremely difficult to control and perform since sudden catastrophic failure in any one of several failure modes possible in sandwich structures can impair accurate determination of the mode in which failure initiates. While theoretical-experimental correlation has been shown to be surprisingly good in some cases, it has been shown to be surprisingly poor in other cases, particularly when honeycomb cores are used. Poor correlation is generally attributed to small initial facesheet imperfections that trigger a flatwise core or core-to-facesheet failure. However, there is strong evidence in the literature that poor theoretical-experimental correlation of the wrinkling stress in sandwich structures with

honeycomb cores is due to lack of validity during test of one or more of the basic assumptions, listed in Table 2, that facesheet wrinkling theory is generally based upon. Test results reported for sandwich struts having (1) predicted wrinkling wavelengths greater than the core cell size, (2) predicted facesheet dimpling loads much higher than the predicted wrinkling loads, and (3) predicted antisymmetric buckling loads much higher than the wrinkling loads generally show correlation with theoretical predictions to within 20% or better.

Initial facesheet imperfections can seriously lower facesheet failure loads. Analyses incorporating the effects of initial facesheet waviness generally rely on a parameter that characterizes the amplitude of this waviness. Attempts have been made to measure this parameter directly; however, the best results have been obtained when the parameter is determined empirically from a large number of destructive tests. These tests should include the effects of combined loads, especially in the case of sandwich structures with anisotropic facesheets. Rigorous theoretical and experimental treatment of the wrinkling of sandwich panels subject to combined loads is conspicuously absent from the literature.

There are many ways in which the state-of-the-art of predicting facesheet wrinkling loads in sandwich structures may be advanced. Among the effects that should be investigated further are:

1. The effects of initial imperfections in the symmetric *and* the antisymmetric mode.
2. The effects of combined loads.
3. The effects of facesheet bending-twisting coupling.
4. The effects of facesheet transverse shear flexibility.

SECTION 4

REFERENCES

1. Plantema, F. J., *Sandwich Construction,* John Wiley and Sons, New York, 1966.

2. Timoshenko, S. P. and Gere, J. M., *Theory of Elastic Stability,* McGraw-Hill, New York, 1961.

3. Allen, H. G., *Analysis and Design of Structural Sandwich Panels,* Pergamon Press, Oxford, 1969.

4. Gough, G. S., Elam, C. F., and de Bruyne, N. D., "The Stabilization of a Thin Sheet by a Continuous Supporting Medium," *Journal of the Royal Aeronautical Society,* Vol. 44, 1940, pp. 12-43.

5. Williams, D., Leggett, D. M. A., and Hopkins, H. G., "Flat Sandwich Panels Under Compressive End Loads," ARC Technical Report R&M 1987, 1941.

6. Cox, H. L. and Riddell, J. R., "Sandwich Construction and Core Materials III: Instability of Sandwich Struts and Beams," ARC Technical Report R&M 2125, 1945.

7. Hoff, N. J. and Mautner, S. E., "Buckling of Sandwich-Type Panels," *Journal of the Aeronautical Sciences,* Vol. 12, 1945, pp. 285-297.

8. Williams, D., "Sandwich Construction: A Practical Approach for the Use of Designers," RAE Report No. Structures 2, 1947.

9. Hemp, W. S., "On a Theory of Sandwich Construction," ARC Technical Report R&M 2672, 1948.

10. Hexcell Corporation, "The Basics of Bonded Sandwich Construction," TSB 124, 1986.

11. Norris, C. B., Erickson, W. S., March, H. W., Smith, C. B., and Boller, K. H., "Wrinkling of the Facings of Sandwich Constructions Subjected to Edgewise Compression," FPL Report No. 1810, 1949.

12. Norris, C. B., Boller, K. H., and Voss, A. W., "Wrinkling of the Facings of Sandwich Constructions Subjected to Edgewise Compression," FPL Report No. 1810-A, 1953.

13. Goodier, J. N. and Neou, I. M., "The Evaluation of Theoretical Critical Compression in Sandwich Plates," *Journal of the Aeronautical Sciences,* Vol. 18, 1951, pp. 649-656, 664.

14. Goodier, J. N. and Hsu, C. S., "Nonsinusoidal Buckling Modes of Sandwich Plates," *Journal of the Aeronautical Sciences,* Vol. 21, 1954, pp. 525-532.

15. Yusuff, S., "Theory of Wrinkling in Sandwich Construction," *Journal of the Royal Aeronautical Society,* Vol. 59, 1955, pp. 30-36.

16. Pearce, T. R. A. and Webber, J. P. H., "Buckling of Sandwich Panels with Laminated Face Plates," *Aeronautical Quarterly,* Vol. 23, 1972, pp. 148-160.

17. Webber, J. P. H. and Stewart, I. B., "A Theoretical Solution for the Buckling of Sandwich Panels With Laminated Face Plates Using a Computer Algebra System," Report No. 407, University of Bristol, 1989.

18. Gutierrez, A. J. and Webber, J. P. H., "Flexural Wrinkling of Honeycomb Sandwich Beams with Laminated Faces," *International Journal of Solids and Structures,* Vol. 16, 1980, pp. 645-651.

19. Shield, T. W., Kim, K. S., and Shield, R. T., "The Buckling of an Elastic Layer Bonded to an Elastic Substrate in Plane Strain," *Journal of Applied Mechanics,* Vol. 61, 1994, pp. 231-235.

20. Jenkinson, P. M. and Kuenzi, E. W., "Wrinkling of the Facings of Aluminum and Stainless Steel Sandwich Subjected to Edgewise Compression," FPL Report No. 2171, 1959.

21. Harris, B. J. and Crisman, W. C., "Face Wrinkling Mode of Buckling of Sandwich Panels," *ASCE Journal of the Engineering Mechanics Division,* Vol. 91, 1965, pp. 93-111.

22. Department of Defense, "Structural Sandwich Composites," MIL-HNDBK-23A, Washington, DC, 1968.

23. Pearce, T. R. A. and Webber, J. P. H., "Experimental Buckling Loads of Sandwich Panels With Carbon Fibre Face Plates," *Aeronautical Quarterly,* Vol. 24, 1974, pp. 295-312.

24. Camarda, C. J., "Experimental Investigation of Graphite Polyimide Sandwich Panels in Edgewise Compression," NASA TM-81895, 1980.

25. Bansemir, H. and Pfeifer, K., "Local Stability of Sandwich Structures With Thin Fiber Reinforced Face Skins for Space Application," *Proceedings of the SAMPE European Chapter Third Technology Conference London, England*, 1983, pp. 421-426.

26. Yusuff, S., "Face Wrinkling and Core Strength in Sandwich Construction," *Journal of the Royal Aeronautical Society,* Vol. 64, 1960, pp. 164-167.

27. Rogers, C. W., "Face Wrinkling As a Function of Surface Waviness," Report ERR-FW-196, General Dynamics Corp., 1964.

28. Wan, C. C., "Face Buckling and Core Strength Requirements in Sandwich Construction," *Journal of the Aeronautical Sciences,* Vol. 14, 1947, pp. 531-539.

29. Sullins, R. T., Smith, G. W., and Spier, E. E., "Manual for Structural Stability Analysis of Sandwich Plates and Shells," NASA CR-1457, 1969.

30. Bruhn, E. F., *Analysis and Design of Flight Vehicle Structures,* Tri-State Offset Company, 1973, pp. C12.1-C12.52.

REPORT DOCUMENTATION PAGE

Form Approved
OMB No. 0704-0188

1. AGENCY USE ONLY (Leave blank)	2. REPORT DATE	3. REPORT TYPE AND DATES COVERED
	January 1999	Contractor Report

4. TITLE AND SUBTITLE
Facesheet Wrinkling in Sandwich Structures

5. FUNDING NUMBERS
529-10-11-01
NAS1-19347, Task 13

6. AUTHOR(S)
Robert P. Ley, Weichuan Lin, and Uy Mbanefo

7. PERFORMING ORGANIZATION NAME(S) AND ADDRESS(ES)
Northrop Grumman Corporation
Military Aircraft Systems Division
One Hornet Way
El Segundo, CA 90245-2804

8. PERFORMING ORGANIZATION REPORT NUMBER

9. SPONSORING/MONITORING AGENCY NAME(S) AND ADDRESS(ES)
National Aeronautics and Space Administration
Langley Research Center
Hampton, VA 23681-2199

10. SPONSORING/MONITORING AGENCY REPORT NUMBER
NASA/CR-1999-208994

11. SUPPLEMENTARY NOTES
Langley Technical Monitor: Juan R. Cruz

12a. DISTRIBUTION/AVAILABILITY STATEMENT
Unclassified-Unlimited
Subject Category 39 Distribution: Nonstandard
Availability: NASA CASI (301) 621-0390

12b. DISTRIBUTION CODE

13. ABSTRACT (Maximum 200 words)

The purpose of this paper is to provide a concise summary of the state-of-the-art for the analysis of the facesheet wrinkling mode of failure in sandwich structures. This document is not an exhaustive review of the published research related to facesheet wrinkling. Instead, a smaller number of key papers are reviewed in order to provide designers and analysts with a working understanding of the state-of-the-art. Designers and analysts should use this survey to guide their judgment when deciding which one of a wide variety of available facesheet wrinkling design formulas is applicable to a specific design problem.

14. SUBJECT TERMS	15. NUMBER OF PAGES
Sandwich Structures, Facesheet Wrinkling, Honeycomb Core, Foam Core	49
	16. PRICE CODE: A03

17. SECURITY CLASSIFICATION OF REPORT	18. SECURITY CLASSIFICATION OF THIS PAGE	19. SECURITY CLASSIFICATION OF ABSTRACT	20. LIMITATION OF ABSTRACT
Unclassified	Unclassified	Unclassified	UL